



**DANIEL ENRIQUE GUAUQUE MELLADO**

**EVAPOTRANSPIRATION AND WATER BALANCE IN THE  
NEOTROPICAL FOREST OF SOUTHEASTERN BRAZIL**

**LAVRAS-MG**

**2021**

**DANIEL ENRIQUE GUAUQUE MELLADO**

**EVAPOTRANSPIRAÇÃO E COMPORTAMENTO DO BALANÇO HÍDRICO EM  
UM FRAGMENTO DE MATA ATLÂNTICA**

Dissertação apresentada à Universidade Federal de Lavras,  
como parte das exigências do Programa de Pós-Graduação em  
Recursos Hídricos, área de concentração em Hidrologia, para  
obtenção do título de Mestre.

Orientador

Prof. Dr. Carlos Rogério de Mello

Co-orientador

Profa. Dra. Sílvia de Nazaré Monteiro Yanagi

**LAVRAS-MG**

**2021**

**Ficha catalográfica elaborada pelo Sistema de Geração de Ficha Catalográfica da Biblioteca Universitária da UFLA, com dados informados pelo(a) próprio(a) autor(a).**

Mellado, Daniel Enrique Guauque.

Evapotranspiration and Water Balance in the Neotropical Forest of Southeastern Brazil / Daniel Guauque Mellado. - 2021.

68 p. :il.

Orientador(a): Carlos Rogério de Mello.

Coorientador(a): Silvia de Nazaré Monteiro Yanagi.

Dissertação (mestrado acadêmico) - Universidade Federal de Lavras, 2021.

Bibliografia.

1. Biophysical controls. 2. Soil water storage. 3. Space-time analysis. I. de Mello, Carlos Rogério. II. Yanagi, Silvia de Nazaré Monteiro. III. Título.

**DANIEL ENRIQUE GUAUQUE MELLADO**

**EVAPOTRANSPIRATION AND WATER BALANCE IN A NEOTROPICAL FOREST  
OF SOUTHEASTERN BRAZIL**

Dissertação apresentada à Universidade Federal de Lavras,  
como parte das exigências do Programa de Pós-Graduação em  
Recursos Hídricos, área de concentração em Hidrologia, para  
obtenção do título de Mestre.

Aprovada em 29 de março de 2021.

Prof. Dr. Carlos Rogério de Mello (PPGRH/UFLA)

Prof. Dr. Adriano Valentim Diotto (PPGRH/UFLA)

Prof. Dr. Jorge Alberto Guzman Jaimes. (ABE – University of Illinois)



Orientador

Prof. Dr. Carlos Rogério de Mello

Co-orientador

Profa. Dra. Sílvia de Nazaré Monteiro Yanagi

**LAVRAS-MG**

**2021**

*Dedico este trabajo a todos los pesquisidores que, con esfuerzo, día a día entregan parte de su tiempo y tranquilidad, solucionando problemáticas de diversas índoles, en la búsqueda constante de opciones de mejora en todos los campos. Esto a pesar de las marcadas limitaciones y falta de interés de los gobiernos por la ciencia y tecnología, que tristemente vienen desvalorizando el trabajo científico en América Latina y el mundo.*

## AGRADECIMENTOS

A Deus por ser sempre minha guia e o valor para fazer todo possível.

Agradeço ao Brasil e a sua gente, por me acolher e brindar apoio em tempos difíceis, principalmente entre a pandemia do CODVID-19.

À Universidade Federal de Lavras e ao Departamento de Recursos Hídricos, pela oportunidade oferecida para nós os estrangeiros de cumprir nossos sonhos.

Ao Professor Carlos Rogério de Mello, pela oportunidade e apoio, confiança depositada em mim, compreensão e constante orientação. Fico totalmente agradecido pelo que fez, e estarei sempre orgulhoso de mencionar seu nome.

À Professora Sílvia de Nazaré Monteiro Yanagi e aos Doutorandos Vanessa Alves Mantovani e André Ferreira Rodrigues pela disposição e colaboração no desenvolvimento deste trabalho.

A todos meus companheiros do Laboratório de Hidrologia Florestal, aos alunos de iniciação científica e servidores técnicos e demais pessoas que contribuíram na captura e processamento de dados para o desenvolvimento desta pesquisa.

A todos os professores do departamento que contribuíram para a minha formação pessoal e intelectual.

A todos os colegas de Pós-graduação, por acompanhar nossas lutas e por sua amizade.

A meus pais, Leonilde e Ernesto por me colocar sempre em suas orações e apoiar em diferentes formas meus sonhos e todas minhas decisões.

À Vivian e João por ser uma das grandes razões de estar aqui, pelas manhãs de café e noites de vinho, por sua compreensão e orientação psicológica, entre muitos outros aspectos.

À república Curi por me apoiar nos inícios desta viagem, quando passei momentos complicados. Também aos caras do Apto 102 por sua amizade.

À CAPES pela concessão de bolsas para o desenvolvimento deste trabalho.

**MUCHAS GRACIAS!**

## RESUMO

As florestas da Mata Atlântica brasileira são ecossistemas de alta importância por seus inumeráveis serviços ambientais oferecidos, sendo classificadas pela UNESCO como uma das mais importantes reservas da biosfera mundial. Porém, são ecossistemas altamente impactados e ameaçados pelas pressões antropogênicas. O objetivo deste estudo foi avaliar a evapotranspiração e os componentes do balanço hídrico em um fragmento remanescente de Mata Atlântica (AFR) semidecidua, com base em informações hidrometeorológicas oriundas de 7 anos hidrológicos (2014-2020) de monitoramento. A finalidade principal foi analisar e modelar os padrões espaço-temporais da evapotranspiração e seus controles biofísicos, assim como componentes do balanço hídrico: interceptação da chuva pelo dossel, umidade do solo e os diferentes fluxo de água, para compreender a dinâmica hidrológica nesta floresta. Em média, dos sete anos hidrológicos estudados, a interceptação das chuvas pelo dossel foi significativa e correspondeu a 19% da precipitação (P), enquanto a evapotranspiração correspondeu a 77%. O processo de transpiração é controlado pelos estômatos e pela umidade do solo, principalmente nos períodos de seca. Com base nas análises do balanço hídrico, o fluxo de água abaixo da zona radicular (DP) apresentou variação entre 3% e 49% da P, apresentando uma redução na recarga de água nas camadas mais profundas do solo. Portanto, a pesar das limitações de água no período de análise, a floresta neotropical se destacou como um elemento chave para prover funções ecológicas e para o controle e reserva de água.

**Palavras chaves:** armazenamento de água no solo, controles biofísicos, interceptação de chuva, análise espaço-temporal.

## ABSTRACT

The Atlantic Forest ecosystems have a high relevance due to their numerous ecosystem services. UNESCO understands it as one of the most critical biospheres reserves globally. However, these ecosystems have been threatened by anthropogenic pressures. This study evaluated the evapotranspiration and the water balance components in a remaining fragment of the Atlantic Forest (AFR) based on hydrometeorological datasets from seven hydrological years (2014-2020). The focus was to analyze and model the spatial and temporal patterns of evapotranspiration and their biophysical controls, the water balance components of the canopy rainfall interception, soil moisture, and the different pathways of the water. The rainfall canopy interception was significant, accounting for 19% of total gross precipitation (P). In contrast, evapotranspiration accounted for an average of 77% of P. The processes involved with evapotranspiration are controlled by stomatal and soil water storage, mainly in the dry periods. Based on the water balance analysis, the water that flows below the root zone (DP) showed a variation between 3% and 49% of P. Therefore, despite the water limitations during the analyzed period, the Neotropical Forest stands out as a critical element to provide ecological functions, mainly for controlling and storage water.

**Keywords:** soil water storage, biophysical controls, rainfall interception, space-time analysis.

## LISTA DE FIGURAS

Figure 1 - Geographical location and instrumentation used for hydrometeorological monitoring elements in the Atlantic Forest experimental area, in southeastern Brazil. ....	37
Figure 2 - Average daily (a) gross precipitation (P), (b) daily mean air temperature ( $T_a$ ), (c) daily global solar radiation ( $R_s$ ), (d) deficit of vapor pressure deficit (DVP), and (e) relative extractable water (REW) in the 0–1.0-m soil layer. Shaded columns represent periods of wet seasons.....	45
Figure 3 - Monthly gross precipitation (P) and canopy rainfall interception (C) (a), monthly effective (or net) precipitation (NP), with respective standard deviations (vertical bars) (b), monthly soil water storage variation in the 0-1.0 m control layer ( $\Delta S$ ), with respective standard deviations (vertical bars) (c). Shaded columns represent periods of wet seasons.....	46
Figure 4 - Spatial patterns of daily average evapotranspiration in the dry period: (i) multiannual variability (average from 2014 to 2020); (ii) interannual variability.....	49
Figure 5 - Annual modeled data of (a) daily energy flux: net radiation, sensible heat flux and soil heat flux ( $R_n$ , H and G; left scale); (b) latent heat flux ( $\lambda E$ , left scale) and equivalent evapotranspiration in millimeters (E, right scale); (c) daily coefficient of Priestley-Taylor ( $\alpha = \lambda E / \lambda E_{eq}$ , left scale); (d) daily canopy conductance ( $g_s$ , left scale); and (e) daily decoupling factor ( $\Omega$ , left scale). Shaded columns represent periods of wet seasons.....	50
Figure 6 - Relationship between modeled evapotranspiration (EPM) and evapotranspiration from water balance (EWB) and precision statistics (RMSE e NS).....	52
Figure 7 - Monthly water balance components: (a) Gross precipitation (P); (b) evapotranspiration (EPM); (c) water storage variation ( $\Delta S$ ) in root zone; and (d) the water flux below the root zone (Dr) for the seven hydrological studied years (2014 to 2020). .....	53
Figure 8 - Relationships between average observed gross rainfall (P): (a) throughfall (TF); (b ) stemflow; (c) C/P ratio (Stf); and (d) real evapotranspiration (E). .....	54
Figure 9 - Relationships between vapor pressure deficit (VPD, left column) with (a) daily modeled evapotranspiration and (b) daily $g_s$ .....	56
Figure 10 - Relationship between the monthly mean values of the Priestley-Taylor ( $\alpha = \lambda E / \lambda E_{eq}$ ) coefficient and the relative extractable soil water content (REW) (a. 0.10 m; b. 0.20 m; c. 0.30 m; d. 0.40 m; and e. 1.0 m). .....	57

**LISTA DE TABELAS**

Table 1 - Daily average of gross precipitation (P, mm d-1), throughfall (TF, mm d-1), streamflow (Stf, mm d-1) and canopy rainfall interception in the dry and wet periods of the hydrological years from 2014 to 2020.....	47
Table 2 - Daily average evapotranspiration of the dry periods (EWB, mm d-1), the coefficient of variation (CV, %) between the points of the water balance, and precision statistics of the semivariogram model fitted.....	48
Table 3 - Daily average values of net radiation (Rn, MJ m-2 d-1), latent heat flux (LE, MJ m-2 d-1), sensible heat flux (H, MJ m-2 d-1), soil heat flux (G, MJ m-2 d-1), latent heat flux ( $\lambda E_{res}$ , MJ m-2 d-1), coefficient of Priestley-Taylor ( $\alpha = \lambda E / \lambda E_{eq}$ ), canopy conductance (gs, mm s-1), decoupling factor ( $\Omega$ ) and evapotranspiration (E, mm d-1) in the dry, wet and annual time scales of the hydrological years from 2014 to 2020.....	51

## SUMÁRIO

<b>PRIMEIRA PARTE .....</b>	<b>13</b>
<b>1 INTRODUÇÃO GERAL .....</b>	<b>13</b>
<b>2 REFERENCIAL TEÓRICO .....</b>	<b>13</b>
<b>2.1 O Bioma Mata Atlântica .....</b>	<b>15</b>
<b>2.2 Hidrologia Florestal.....</b>	<b>16</b>
<b>2.3 Balanço Hídrico .....</b>	<b>17</b>
<b>2.4 Balanço de energia.....</b>	<b>20</b>
<b>2.5 Evapotranspiração Florestal .....</b>	<b>21</b>
<b>2.6 Controles biofísicos da evapotranspiração.....</b>	<b>24</b>
<b>4 CONSIDERAÇÕES GERAIS .....</b>	<b>27</b>
<b>5 REFERÊNCIAS BIBLIOGRÁFICAS .....</b>	<b>28</b>
<b>SEGUNDA PARTE – ARTIGO: EVAPOTRANSPIRAÇÃO E COMPORTAMENTO DO BALANÇO HÍDRICO EM UM FRAGMENTO DE MATA ATLÂNTICA .....</b>	<b>34</b>
<b>1 INTRODUCTION .....</b>	<b>35</b>
<b>2 MATERIAL AND METHODS .....</b>	<b>36</b>
<b>2.1 Site description.....</b>	<b>36</b>
<b>2.2 Water balance monitoring .....</b>	<b>38</b>
<b>2.3 Meteorological and LAI measurements .....</b>	<b>39</b>
<b>2.4 Elements of the water balance calculation .....</b>	<b>40</b>
<b>2.5 Parameterization of the evapotranspiration model and components.....</b>	<b>41</b>
<b>2.6 Spatial modeling and precision statistics.....</b>	<b>43</b>
<b>3 RESULTS .....</b>	<b>44</b>
<b>3.1 Meteorological conditions observed in the studied period .....</b>	<b>44</b>
<b>3.2 Precipitation partitioning and soil water storage behavior in the studied period</b>	<b>46</b>
<b>3.3 Modeling and spatiotemporal patterns of evapotranspiration.....</b>	<b>48</b>
<b>3.4 Water balance .....</b>	<b>52</b>
<b>4 DISCUSSION.....</b>	<b>53</b>
<b>5.1 Precipitation partitioning and soil water storage behavior .....</b>	<b>53</b>
<b>5.2 Modeling and spatiotemporal patterns of evapotranspiration.....</b>	<b>55</b>

<b>5.3</b>	<b>Water balance .....</b>	<b>58</b>
<b>5</b>	<b>CONCLUSIONS.....</b>	<b>59</b>
	<b>REFERENCES .....</b>	<b>61</b>
	<b>APÊNDICE A – Variáveis complementares do modelo PM .....</b>	<b>68</b>

## **PRIMEIRA PARTE**

### **1 INTRODUÇÃO GERAL**

Depois da precipitação, a evapotranspiração é o principal componente do balanço hidrológico terrestre, sendo seu entendimento, fundamental para a avaliação dos recursos hídricos e políticas sustentáveis de gestão da água. De forma geral, no ciclo hidrológico, a evapotranspiração (E) representa em torno de 70% da precipitação (TAN et al., 2019). Este processo é responsável por transferir a umidade da superfície da Terra para a atmosfera na forma de vapor. Devido às complexas interações entre fatores meteorológicos e fatores específicos do local de estudo, a evapotranspiração é de difícil quantificação, sendo que para modelagem do balanço hídrico, é imprescindível sua estimativa temporal e espacial (ZHAO et al., 2013).

Consequência do aumento dos gases de efeito estufa (GEE), o aquecimento global pode aumentar a variabilidade das precipitações e a probabilidade de secas. Em consequência, compreender as dinâmicas do balanço hídrico e em especial, da evapotranspiração, em nível ecossistêmico, será cada vez mais importante para a gestão dos recursos hídricos em escalas locais e regionais (ABDOLLAHI; BAZARGAN; MCKAY, 2019). No mundo, foram realizados diferentes estudos para a quantificação da evapotranspiração em ecossistemas naturais (PEREIRA et al., 2010; KUME et al., 2011; CABRAL et al., 2015; MARQUES et al., 2020; IIDA et al., 2020). Porém, apesar da importância ambiental e ecológica das florestas neotropicais, são poucos os estudos que detalham seu funcionamento hidrológico, principalmente em relação ao balanço hídrico e à evapotranspiração.

Dentro das florestas neotropicais do Brasil, as Florestas Estacionais Semideciduais de Montana desempenham um papel chave no sistema climático global (TAFFARELLO et al., 2017) e se encontram entre os pontos críticos (*hot spots*) do mundo para manutenção da biodiversidade (DA SILVA et al., 2020; REZENDE et al., 2018). Este ecossistema originalmente possuía 131 milhões de hectares, sendo considerado uma das maiores florestas tropicais da América. Porém, na atualidade, em consequência do desmatamento, as mudanças no uso do solo e da exploração intensiva de recursos naturais, possui apenas o 28% de sua cobertura original, sendo que Minas Gerais foi o estado que mais desmatou entre 2017 e 2018 (com uma taxa de 29,79%) (SOS Mata Atlântica; INPE, 2019).

Analisando o panorama futuro das florestas de Mata Atlântica, existe uma grande necessidade de diminuir seu desmatamento progressivo, já que esta prática pode acentuar as

mudanças micro e macro climáticas, que comprometem as dinâmicas ecossistêmicas e hidrológicas, afetando habitats e contribuindo para a degradação ambiental. Deste modo, estudar o balanço hídrico e o comportamento da evapotranspiração nestes ecossistemas é importante para subsidiar estratégias que levem à sua conservação e uso racional.

Apesar dos estudos de evapotranspiração e balanço hídrico realizados em florestas de Mata Atlântica (PEREIRA et al., 2010; FELTRIN et al., 2011; SALEMI et al., 2013; MELLO et al., 2019), ainda faltam conhecimentos detalhados sobre a variabilidade espaço-temporal da evapotranspiração em pequenos remanescentes, e sua influência com as variáveis meteorológicas interativas, composição e fenologia da vegetação e condições da água no solo. Ademais, o particionamento de energia no ecossistema e os controles biofísicos da evapotranspiração são fatores importantes e que afetam diretamente a evapotranspiração. A maioria dos estudos realizados em florestas deste tipo foram realizados em períodos inferiores a 2 anos e não foram retratados eventos climáticos extremos (especialmente secas prolongadas e chuvas concentradas), e nem alterações nos padrões anuais do balanço hídrico e energético no ecossistema.

Estudos eco-hidrológicos foram realizados em outros ecossistemas no Brasil, através de medições diretas do fluxo da evapotranspiração, mediante o sistema “Eddy Covariance” (e.g. DA ROCHA et al., 2004; MARQUES et al., 2020; CABRAL et al., 2015), uma técnica de covariância dos vórtices turbulentos, que mede a transferência de massa e energia e interação superfície-atmosfera. Todavia, este sistema é muito complexo e de alto custo. Porém, Jones et al. (2017) mencionam que existem metodologias efetivas para o cálculo indireto da evapotranspiração, como o balanço de energia e o balanço hídrico com enfoque residual, que tem sido amplamente usado por sua efetividade. Assim, mesmo modelos de evapotranspiração, tais como, os modelos de folha grande ou Penman-Monteith (PM), validados em função de medições observadas *in situ*, são capazes de capturar a variabilidade do clima e da água no solo, sendo muito adequados para fazer cálculos de balanço hídrico em florestas (KUME et al., 2011).

Nesse sentido, objetiva-se nesta pesquisa, analisar e modelar os padrões espaço-temporais da evapotranspiração e seus controles biofísicos, e avaliar os componentes do balanço hídrico em um período de 7 anos hidrológicos (2014 a 2020).

## 2 REFERENCIAL TEÓRICO

### 2.1 O Bioma Mata Atlântica

A Organização das Nações Unidas para a Educação, a Ciência e a Cultura (UNESCO) reconheceu a Mata Atlântica como uma das mais importantes reservas da biosfera em nível mundial, devido à sua alta diversidade e endemismos, assim como por sua relevância ambiental e hidrológica (MELLO et al., 2019). Este Bioma sustenta mais do 60% da população urbana do Brasil, o que tem refletido nos últimos séculos em diferentes graus de pressão sobre o mesmo, causando diminuição da cobertura vegetal, fragmentação das florestas e, consequentemente, impactos no regime climático e hidrológico (SCARANO; CEOTTO, 2015; ZANINI et al., 2021). Segundo Taffarello et al. (2017) e Macedo et al. (2021) os ecossistemas de Mata Atlântica têm sido destacados devido à sua importância como prestadores de serviços ambientais, sendo estratégicos para mitigar os efeitos de secas persistentes. Todavia, na atualidade o bioma possui apenas 28% de sua cobertura original, considerado um dos pontos críticos (*hot spots*) da biodiversidade (DA SILVA et al., 2020; REZENDE et al., 2018). Segundo o INPE (2019), no ecossistema da Mata Atlântica, entre 2017 e 2018, foram destruídos 11.399 ha (113 km<sup>2</sup>), sendo os estados de Minas Gerais (29,79%), Paraná (18,07%), Piauí (18,52%), Bahia (17,50%) e Santa Catarina (8%) os que apresentaram maiores índices de desmatamento.

As florestas de Mata Atlântica são ecossistemas muito frágeis, sendo que 85% destas têm baixa capacidade de resiliência (TAMBOSI et al., 2014). Além disso, na atualidade, mais de 90% dos remanescentes são afetados por processos contínuos de fragmentação e aproximadamente 46% destes, se encontram afetados por um forte efeito de borda (MACEDO et al., 2021; POORTER et al., 2016). Assim, é relevante conhecer as dinâmicas hidrológicas aportadas nestes ecossistemas, a fim de subsidiar estratégias para sua conservação e uso racional.

A área do presente estudo consiste em um remanescente de Floresta Estacional Semidecidual de Montana (AFR) com área de 6,3 ha (dentro o bioma de Mata Atlântica), que faz parte do Laboratório de Pesquisas Florestais da Universidade Federal de Lavras (UFLA) (JUNQUEIRA et al., 2017). Nesta área, é realizado monitoramento periódico da vegetação, mediante censo florestal realizado desde 1994, onde são medidas as mudanças no crescimento das espécies, a mortalidade, dentre outras variáveis dendrométricas. Desde o ano 2012, realiza-se o monitoramento constante dos elementos do balanço hídrico como a precipitação (externa,

interna e o escoamento pelo tronco) e umidade no solo e também de variáveis meteorológicas (temperatura ( $T_a$ ), umidade relativa (RH), saldo de radiação solar ( $R_n$ ), pressão barométrica ( $P_a$ ), velocidade (WS) e direção do vento (DW)) e do índice de área foliar (LAI).

Neste remanescente de Mata Atlântica tem sido conduzidas diferentes pesquisas hidrológicas tais como: (i) Junqueira et al. (2017) estudaram a estabilidade temporal do teor de água do solo entre junho de 2013 e março de 2015, estudando as relações entre a precipitação e umidade do solo, assim como a relação entre os indicadores da paisagem e sua estabilidade no tempo; (ii) Terra et al. (2018) estudaram o comportamento espaço-temporal do escoamento pelo tronco, entre abril de 2016 e março de 2017, amostrando o efeito das características da floresta neste elemento do balanço hídrico, ademais sua correlação com a umidade do solo; (iii) Junqueira et al. (2019) modelaram o processo de interceptação florestal no fragmento de Mata Atlântica para o período de setembro de 2012 a março de 2015, analisando o comportamento da interceptação sobre condições de seca (nos anos hidrológicos de 2014 e 2015) e sua relação com as características da floresta; (iv) Rodrigues et al. (2020) estudaram o comportamento espaço-temporal do conteúdo de umidade no solo e precipitação efetiva nos anos hidrológicos 2014 e 2015, trabalhando a relação com a topografia e características semidecíduas da floresta. Assim, ainda não foi realizado um estudo que caracterize e modele a evapotranspiração e represente o balanço hídrico anual da floresta neste fragmento de Mata Atlântica, estudo que pode contribuir ao entendimento da dinâmica fisiológica da floresta sobre diferentes condições climáticas e sua relação com as respostas hidrológicas nestas áreas, especialmente sob anos hidrológicos abaixo da média climatológica.

## **2.2 Hidrologia Florestal**

Dos ecossistemas terrestres, as florestas cumprem uma função essencial no aporte de serviços, principalmente, no tocante à proteção de nascentes e recarga subterrânea, fornecendo água para o consumo humano. As florestas apresentam estreita relação com o ciclo hidrológico, sendo considerada a ocupação do solo que mais beneficia os recursos hídricos, já que provocam o retardamento do movimento da água da chuva, em direção aos cursos d'água, por meio do processo de interceptação, absorção e transpiração. Além disso, minimizam os efeitos de lixiviação de nutrientes do solo e o assoreamento dos corpos d'água (ELLISON et al., 2017).

Sheil (2018) infere que as florestas devem ser conservadas por sua eficácia para estabilizar e manter o regime hídrico de uma região, já que melhoram a estrutura do solo, favorecendo os processos de infiltração e percolação, além de atenuar o escoamento superficial

direto. A floresta nativa desempenha importância na formação de novas massas atmosféricas úmidas como consequência dos processos de interceptação pelo dossel e evapotranspiração, os quais contribuem para o processo de precipitação. Além disso, contribuem melhorando as condições para o armazenamento de água no solo (FRIESEN; LUNDQUIST; VAN STAN, 2015).

Nesse sentido, os estudos hidrológicos nas florestas são importantes para o entendimento da dinâmica dos fluxos de água, e no âmbito da planificação e manejo das bacias hidrográficas, uma vez que alterações na cobertura vegetal, interferem nas trocas gasosas bem como nos atributos físicos do solo, que refletem no regime hídrico dos mananciais.

### **2.3 Balanço Hídrico**

O balanço hídrico é uma análise dos componentes do ciclo hidrológico resultante da aplicação dos princípios de conservação de massa, em um volume de solo com presença de cobertura vegetal, em um tempo determinado, apresentando o fluxo de água (ganhos e perdas) entre as variáveis do sistema e a parcela armazenada (ABDOLLAHI; BAZARGAN; MCKAY, 2019). Essencialmente, as variáveis que inferem como possíveis entradas do sistema são: precipitação (P), irrigação (I) e ascensão capilar (CR); as possíveis variáveis responsáveis pela saída de água compreendem: evapotranspiração (E), escoamento superficial (RO) e drenagem profunda (DP). Dessa maneira, o balanço hídrico do solo pode ser expressado segundo ALLEN et al. (1998), como:

$$\frac{\Delta S}{\Delta T} = \frac{(P + I + CR)}{\Delta T} - \frac{(E + RO + DP)}{\Delta T} \quad (1)$$

Contudo, as abordagens do balanço hídrico dependem da escala de análise e objeto de estudo. Assim, pode-se, por exemplo, analisar o comportamento da evapotranspiração na escala bacia hidrográfica ou áreas específicas de cobertura vegetal (florestas nativas e/ou plantadas), o armazenamento d'água no solo e zona saturada, simular o escoamento superficial, entre outras abordagens (PAKPARVAR et al., 2018). Segundo Almeida e Sands (2016), o balanço hídrico em ecossistemas florestais depende da precipitação, interceptação pelo dossel, evaporação do solo, transpiração das plantas, umidade do solo e drenagem profunda. Cada ecossistema sustenta particularidades de acordo com o regime climático, tipo de solo e características fisiológicas das espécies florestais, assim como sua estrutura, composição e estado de conservação. Por exemplo, em alguns biomas tropicais a principal entrada do balanço hídrico é

a precipitação, entretanto, em biomas áridos as maiores entradas correspondem à ascensão capilar de recargas subterrâneas (ZHAO et al., 2016).

Jones et al. (2017) observaram que os cálculos do balanço hídrico em pequenas áreas florestais, requerem principalmente, medições precisas ou estimativas da precipitação (P), evapotranspiração (E), mudanças no armazenamento de água na zona radicular ( $\Delta S$ ) e fluxo de água abaixo da zona radicular (DP). Dado que são os elementos que melhor descrevem as entradas e saídas hidrológicas, em escala local, simplificando a Eq. 1, tem-se o balanço hídrico como:

$$\frac{E}{\Delta T} = \frac{P - \Delta S - DP}{\Delta T} \quad (2)$$

Portanto, quando não existem medições diretas de uma variável, como por exemplo DP (que gera altos custos e dificuldades em nível de campo para instalar e manter lisímetros, piezômetros e tensiômetros capilares), pode-se calcular este, como o resíduo do balanço hídrico quando os demais elementos são conhecidos (JASSAL et al., 2013). Esta simplificação implica situações em que o DP é positivo, ou seja, a água está se movendo para fora da zona radicular (percolação), e quando o DP é negativo, a água está se movendo para cima na zona radicular (ascensão capilar). Quando o método residual é empregado, são necessárias medições diretas de P,  $\Delta S$  e E (JASSAL et al., 2013; JONES et al., 2017).

Avaliar cada elemento da equação de balanço hídrico requer o levantamento de dados ou estimações que representem fisicamente o mecanismo de transporte dos volumes de água no sistema. O uso de medições contínuas é um desafio, principalmente devido ao monitoramento inconsistente combinado com altos custos e a falta de transparência e acessibilidade aos dados. Geralmente, para quantificar algumas variáveis individuais, são utilizados modelos empíricos ou determinísticos, com ou sem componentes aleatórios ou probabilísticos, que descrevam corretamente o processo (OLIVEIRA et al., 2014). No entanto, em alguns modelos de balanço hídrico, há carência de técnicas adequadas para modelar a evapotranspiração, o que resulta muitas vezes na sua sub ou superestimação. A razão para esta carência é pelo fato de que as variáveis que influem neste processo são de difícil medição pela complexidade das trocas de energia (principalmente na transpiração) e seu acoplamento na escala espacial sobre os ecossistemas (ZHAO et al., 2013).

Atualmente, se incrementou o uso de dados de sensoriamento remoto para realização de diversos estudos do balanço hídrico. Sensores como TRMM, MOD16 e GRACE, que trazem informações de precipitação, evapotranspiração e armazenamento de água no solo,

respectivamente, podem ser essenciais para estudos de modelagem em grandes escalas, mas ao nível microclimático podem gerar diferentes níveis de incerteza, como por exemplo na determinação de processos de intercambio de calor, influência da cobertura vegetal nas resistências aerodinâmica e de dossel, entre outros aspectos. Assim, é necessário realizar estudos com monitoramento, especialmente em áreas florestais onde encontram-se altos graus de variabilidade espacial e temporal em cada componente do balanço.

Alguns estudos foram realizados no sentido de descrever os elementos do balanço hídrico (fluxo de água, interceptação de chuva no dossel, umidade do solo, evapotranspiração e sua interação) em várias situações (JONES et al., 2017; TOR-NGERN et al., 2018; ZHAO et al., 2016), mas são escassos na Mata Atlântica brasileira.

Um desses poucos estudos foi o de Pereira et al. (2010) realizado em um fragmento de floresta na Serra da Mantiqueira, onde se compara a evapotranspiração do balanço hídrico com o modelo de Penman-Monteith. Neste estudo, a evapotranspiração representou 86% do total precipitado e a percolação profunda foi responsável por 13,6%. Os autores concluíram que o modelo de Penman-Monteith fornece bons resultados na estimativa da evapotranspiração real, com aplicação potencial em estudos hidrológicos envolvendo fragmentos de Mata Atlântica desta região.

Outro estudo foi o de Feltrin et al. (2011), onde realizaram o balanço hídrico de um remanescente florestal no Rio Grande do Sul, por meio de Lisímetros, demonstrando que aproximadamente 70% do total de chuva foi usado no processo de evapotranspiração. Assim, a drenagem representou mais de 27% da chuva, demonstrando a importância deste componente no cálculo do balanço hídrico.

Salemi et al. (2013) realizaram um estudo baseado no monitoramento hidrometeorológico durante um ano hidrológico em diferentes coberturas vegetais incluindo a Mata Atlântica. No entanto, neste estudo a evapotranspiração correspondeu a 60% da precipitação, sendo a principal variável de saída do balanço hídrico. Recentemente, Mello et al. (2019) quantificaram o balanço hídrico na Serra da Mantiqueira anos hidrológicos de 2009 a 2011, observando que a evapotranspiração correspondeu em média a 50% da precipitação.

Nesse contexto, é importante realizar estudos específicos do balanço hídrico de acordo com as particularidades hidrológicas, climáticas, edáficas e fisiológicas, além do período do estudo, já que especialmente a evapotranspiração, apresenta variabilidade relevante no ecossistema de Mata Atlântica.

## 2.4 Balanço de energia

O balanço de energia na superfície corresponde à distribuição do saldo de radiação ( $R_n$ ) nos diferentes processos físicos e biológicos que têm lugar na interface superfície-atmosfera (BORGES et al., 2020). Esses processos estão relacionados principalmente com fluxos tais como: calor latente ( $\lambda E$ ), associado à evaporação da água no solo e da superfície vegetada bem como da transpiração das plantas; calor sensível ( $H$ ), associado ao aquecimento do ar próximo da superfície; calor no solo ( $G$ ), que representa a condução de energia no solo; a densidade do fluxo de energia associada com o fluxo de  $\text{CO}_2$  ( $F$ ) e o fluxo de energia armazenada na biomassa e no ar dentro do dossel vegetativo ( $S$ ) (CHOWDHURY, 1988; SILBERSTEIN et al., 2003).

Em conformidade com o princípio de conservação de energia, a equação do balanço de em ecossistemas representa a soma dos fluxos de calor mencionados anteriormente, ou seja:

$$R_n = \lambda E + H + G + F + S \quad (3)$$

Em superfícies com extensa vegetação homogênea, os termos  $F$  e  $S$  são desconsiderados, já que representam uma pequena fração do  $R_n$  diário, comparado com as outras quatro componentes do balanço de energia (ALLEN et al., 1998). Desse modo, a equação 3 pode ser simplificada da seguinte maneira:

$$R_n = \lambda E + H + G \quad (4)$$

Atualmente existem diferentes equipamentos que têm a função de medir os fluxos reais de energia em diferentes escalas temporais. Os mais amplamente utilizados para medir esses fluxos nos ecossistemas são o sistema do balanço de energia da razão de Bowen (BREB), o sistema Eddy Covariance (EC) e os cintilômetros (LIU et al., 2013). Porém, esses equipamentos possuem custo de aquisição e manutenção muito altos e apresentam limitações em sua aplicação nos diferentes ecossistemas, como o BREB, que simula uma cobertura homogênea (ABDOLGHAFORIAN et al., 2017).

Existem metodologias efetivas para o cálculo indireto de  $H$  e  $\lambda E$ , usando a teoria de difusão gradiente, representada como uma analogia de circuito de resistência elétrica da evaporação do solo, atuando em paralelo com a transpiração e a evaporação da chuva interceptada em uma camada de ar de dossel comum (SILBERSTEIN et al., 2003). O enfoque clássico, conhecido como método Bulk Transfer (BT), aplicado para superfícies homogêneas, usa a formulação de transferência em massa de fonte única (com base na Teoria de Similaridade de Monin-Obukhov (MOST) para estimar  $H$ , com temperaturas a nível de referência (sobre o

dossel) e de superfície (BRUTSAERT, 1982). Contudo, outros enfoques, como o proposto por Norman et al. (1995), permitem o cálculo com duas temperaturas em uma camada de ar sobre o dossel. Este enfoque tem sido aplicado em diferentes estudos com abordagem micro-meteorológica que contam com medições em várias camadas no dossel, e em estudos de sensores remotos para a avaliação dos fluxos de energia (KALMA; MCVICAR; MCCABE, 2008; SILBERSTEIN et al., 2003). A partir do cálculo de H, pode-se obter indiretamente o  $\lambda E$  como o termo residual na equação do balanço de energia (Eq. 4).

## 2.5 Evapotranspiração Florestal

A evapotranspiração (E) é um componente importante do ciclo hidrológico e do balanço energético nos ecossistemas florestais que compreende outros processos hidrológicos, como percolação profunda, entre outros. Este processo fornece um elo vital entre os sistemas climático, hidrológico e ecológico, já que é responsável por moldar a umidade e a temperatura atmosférica a diferentes escalas espaciais (YAN et al., 2017).

A troca de água entre a superfície da Terra e a atmosfera é um componente essencial do ciclo hidrológico. Estudos anteriores mostraram que nessa troca a evapotranspiração está intimamente relacionada à disponibilidade de energia, demanda atmosférica e disponibilidade de água no solo.(GENG et al., 2020). A quantificação das taxas de evapotranspiração (E) da Terra não é apenas crítica para entender como o ciclo da água interage entre a superfície do planeta e a atmosfera, mas também é crucial para o gerenciamento sustentável dos recursos hídricos e, portanto, a conservação ecológica e ambiental em regiões suscetíveis à seca. Além disso, a evapotranspiração é usada para avaliar o impacto hidrológico das mudanças climáticas a nível de bacia e região hidrográfica (TABARI; HOSSEINZADEH TALAAE, 2014).

A evapotranspiração inclui dois processos que ocorrem simultaneamente no sistema solo-planta-atmosfera, a evaporação direta da umidade da superfície da Terra (no solo e dossel das plantas) e a troca de vapor d' água, que ocorre dentro das folhas das plantas (JASECHKO et al., 2013). No primeiro destes processos, há consumo de calor latente de evaporação a água líquida é convertida em vapor d'água e removida da superfície do solo e do dossel das plantas. A radiação solar direta e a temperatura do ar ambiente fornecem a energia necessária para este processo. A força motriz para retirar o vapor d'água é a diferença entre a pressão do vapor da superfície e da atmosfera circundante. Portanto, para a avaliação do processo evaporativo  $R_n$ ,  $T_a$ , RH e WS são as variáveis climatológicas a serem consideradas. De acordo com Kool et al. (2014), as perdas de água pela interceptação (C) nas florestas geralmente são pequenas em

comparação com a transpiração, e tendem a ser maiores em períodos secos. Ainda assim, a interceptação em florestas neotropicais pode corresponder até 30% das precipitações em períodos úmidos (JUNQUEIRA et al., 2019).

No caso da evaporação do solo (SE), a disponibilidade de água nas camadas e a cobertura vegetal na superfície correspondem às maiores limitações do processo. Segundo Allen et al. (1998) as precipitações frequentes, irrigação e ascensão capilar em um solo com lençol freático raso mantêm a superfície do solo úmida e facilitam o processo evaporativo. Nos casos em que existe redução das chuvas e a capacidade do solo de conduzir a umidade perto da superfície é reduzida, o conteúdo de água nas camadas superiores diminui e a superfície do solo seca. Nessas circunstâncias, a disponibilidade limitada de água controla a evaporação do solo. Na ausência de qualquer fonte de reabastecimento de água na superfície do solo, a evaporação diminui rapidamente e pode quase cessar completamente.

A presença de floresta nativa em diferentes níveis protege a superfície do solo dos efeitos da radiação solar e do vento e aumenta a superfície ativa, reduzindo significativamente as taxas de evaporação da superfície do solo florestal. O secamento da camada superficial depende da textura do solo e de condições climáticas adequadas, que podem também causar secamento no perfil das camadas mais profundas (KUME et al., 2011).

Por outro lado, o processo de transpiração das plantas (Tr) corresponde à transferência de água para a atmosfera, utilizada nos processos metabólicos necessários ao seu crescimento e desenvolvimento. Este processo segue uma relação força-fluxo que é determinada pela capacidade do sistema de transporte da planta de conduzir água do sistema radicular para as folhas (JASECHKO et al., 2013). Essa transferência é controlada por estruturas microscópicas chamadas estômatos, presentes nas folhas das plantas, as quais, além disso, são responsáveis pela passagem de dióxido de carbono e oxigênio. Na maioria das espécies, os estômatos permanecem abertos durante o dia e fechados à noite, porém este comportamento varia e em condições extremas de estresse hídrico e picos de radiação solar incidente (TAN et al., 2019).

O processo de vaporização ocorre dentro da folha, nos espaços intercelulares, e a troca de vapor com a atmosfera é controlada pela condutância estomática em resposta as condições ambientais de luz, temperatura, concentração de CO<sub>2</sub>, umidade relativa do ar e potencial hídrico foliar. Se considera que mais de 90% de toda a água absorvida do solo é perdida por transpiração e apenas uma pequena fração atende as necessidades fisiológicas da planta (LU et al., 2018).

A transpiração em nível florestal é influenciada por inúmeros fatores climáticos, e.g. Rn, déficit de pressão e saturação de vapor da atmosfera (VPD), fatores fisiológicos (Índice de Área Foliar (LAI), estádio de desenvolvimento, resistência do dossel ( $g_s$ ), e espécies do

conjunto de plantas), disponibilidade de água nas diferentes camadas do solo, entre outros fatores, que geram uma grande variabilidade espacial e temporal da Tr em áreas florestais (MARQUES et al., 2020; TAN et al., 2019).

A evapotranspiração é um elemento fundamental nos ecossistemas florestais, representando a lâmina de água necessária para suprir as necessidades hídricas da vegetação. Mello, Lima e Silva (2004) demonstraram que quando a evapotranspiração real em uma área com eucalipto e pastagem é praticamente igual à potencial, e o consumo de água pelas plantas está diretamente associado ao comportamento da umidade do solo, quando esta atinge aproximadamente 70% da capacidade de campo.

De acordo com a Allen et al. (1998), os processos de evaporação da água interceptada, evaporação do solo e transpiração em florestas ocorrem simultaneamente e não há uma maneira fácil de distinguir entre esses processos. Segundo Kool et al. (2014), vários métodos foram desenvolvidos para estimar a evapotranspiração em florestas e seus componentes, em escalas espaciais e temporais correspondentes. Contudo, os métodos diretos constituem-se de medidores de fluxos turbulentos, como o sistema Eddy Covariance (EC), lisímetros, medidores de fluxo de seiva, controles de umidade no solo e balanço hídrico. Também foram desenvolvidos métodos indiretos, que demandam menos complexidade e baseiam-se na aplicação de métodos matemáticos que usam dados medidos em estações meteorológicas.

Existe um grande número de modelos para estimar a evapotranspiração, que podem ser agrupados em várias categorias, como radiação e energia, balanço de água, transferência de massa, temperatura e métodos combinados. Esses métodos variam muito em termos de complexidade, requisitos de dados e confiabilidade (FORD; HUBBARD; VOSE, 2010). Ainda assim, os métodos EC, balanço hídrico e Penman-Monteith (PM) são os mais aceitos e amplamente usados, sendo este último considerado como um método padrão para o cálculo da evapotranspiração potencial nos diferentes ecossistemas e culturas.

O modelo Penman-Monteith (PM) é uma das abordagens mais amplamente empregadas para a estimativa da evapotranspiração, pois tem uma formulação baseada em processo que utiliza variáveis meteorológicas comumente disponíveis, incluindo  $T_a$ , WS, RH e  $R_n$  (ALLEN et al., 1998). Em sua forma mais simples, este modelo é baseado num modelo do tipo “folha grande” de fonte evaporativa simples, que agrupa a heterogeneidade da superfície da Terra em um único elemento evaporativo. Nesta configuração, nenhuma distinção é feita entre evaporação do solo, evaporação da água interceptada pelo dossel ou transpiração através do dossel (ERSHADI et al., 2015). Todavia, existem outras versões do modelo de PM que foram desenvolvidas, e que discriminam os componentes em várias fontes evaporativas (por exemplo,

solo e dossel), com um modelo de PM formulado em cada camada ou componente (Kume et al., 2011; Mu; Zhao; Running, 2011). Porém, a subdivisão em camadas apresenta muitas limitações na parametrização das diferentes condutâncias (aerodinâmicas e do dossel). Deste modo, o modelo PM de fonte evaporativa única fornece estimativas mais precisas da evapotranspiração que modelos com várias fontes evaporativas (ERSHADI et al., 2015).

Pereira et al. (2010) usaram o modelo de PM de fonte evaporativa única para avaliar a evapotranspiração em um fragmento de Mata Atlântica da Serra da Mantiqueira – MG, e concluíram que o método mostrou bom desempenho com respeito à evapotranspiração real obtida mediante o balanço hídrico. Mais recentemente, Mello et al. (2019) aplicaram a mesma metodologia para outra zona da Serra da Mantiqueira, apresentando uma aplicação potencial em estudos hidrológicos envolvidos em fragmentos deste mesmo ecossistema.

## **2.6 Controles biofísicos da evapotranspiração**

A demanda atmosférica da evapotranspiração controla suas variações temporais no ecossistema, determinando as taxas de evaporação potencial que são influenciadas pelas condições atmosféricas (principalmente  $R_n$ , VPD e  $T_a$ ) e os controles fisiológicos e aerodinâmicos provenientes da superfície terrestre, que regulam os processos de troca de gases por médio da abertura e fechamento dos estômatos e mudanças na rugosidade do dossel (MARQUES et al., 2020).

Em uma superfície vegetada, a capacidade dessa superfície em transferir água na forma de vapor para a atmosfera é definida como condutância de superfície ( $g_s$ ). Este parâmetro é o inverso da resistência de superfície ( $r_s$ ) e pode ser decomposto em termos da soma entre as condutâncias do fluxo de vapor na abertura dos estômatos, da área foliar total, através da cutícula, e da superfície do solo (KELLIHER et al., 1995). Por outro lado, a condutância aerodinâmica ( $g_a$ ) está associada à capacidade de transferência de calor e vapor de água da superfície evaporante para o ar acima do dossel. Esta condutância é inversa da resistência aerodinâmica ( $r_a$ ), a qual depende do perfil logarítmico do vento na superfície vegetada (TAN et al., 2019).

Estudos como os de Li et al. (2019) e Geng et al. (2020) mostram que a transferência de vapor no interior do dossel depende essencialmente da velocidade do vento, ou indiretamente da  $g_a$ , sendo um parâmetro em função da turbulência, que representa as condições físicas do dossel, e o controle da transpiração do dossel como um todo, que pode ser influenciada pelas condições climáticas. A  $g_a$  pode ser obtida com medições em campo da velocidade média do

vento na altura de referência ( $u$ ) e a velocidade de atrito ( $u^*$ ). Contudo, poucos estudos contam com medições diretas de  $u^*$ , sendo que geralmente são usados os métodos alternativos propostos por Allen et al. (1998), usando dados de perfil de vento com base na teoria de similaridade Monin-Obukhov.

Diferentes estudos mostram que a  $g_s$  é controlada pelas variáveis da evaporação como a radiação global e o déficit de pressão de vapor. Porém, a parametrização de  $g_s$  apresenta muitos desafios, pois não é apenas regulada pelo ambiente físico, mas também variando entre as espécies, estado da floresta, manejos realizados, entre outros aspectos. Em florestas tropicais, o  $g_s$  difere muito de outros biomas devido às diferenças nos regimes climáticos prevalecentes (TAN et al., 2019). A determinação desta condutância, geralmente é realizada conhecendo os fluxos de calor latente ( $\lambda E$ ) e sensível ( $H$ ) no ecossistema, a partir do modelo inverso da Equação de Penman-Monteith (PM). No entanto, existem modelos físicos para simular este parâmetro, como o modelo multiplicativo de Jarvis (1976), que se baseia em funções multiplicativas de variáveis como umidade do solo, índice de área foliar, dentre outros, o que limita sua aplicação já que implica em um maior número de dados e geralmente necessita de dados reais para ser validado (ERSHADI et al., 2015).

Por outro lado, para conhecer as relações da biosfera-atmosfera, McNaughton e Jarvis (1983) desenvolveram o conceito do fator de desacoplamento ( $\Omega$ ), um indicativo da interação entre a superfície vegetada e atmosfera nos processos de evapotranspiração (MARQUES et al., 2020). Mediante este índice pode-se determinar o grau de acoplamento entre o dossel florestal e atmosfera, onde se a taxa de transpiração é controlada principalmente pelo VPD e a  $g_s$ , se estabelece um forte acoplamento, ou se pelo contrário, é controlado por fatores climáticos como a  $R_n$ , se estabelece um fraco acoplamento (YAN et al., 2017).

Cabe ressaltar que  $\Omega$  é uma variável adimensional que varia entre 0 e 1, sendo que  $\Omega \approx 0$  representa um total acoplamento da superfície com a atmosfera, indicando que a evapotranspiração é principalmente controlada por fatores fisiológicos da floresta. Contrário ao anterior, quando  $\Omega \approx 1$ , a superfície está completamente desacoplada das condições aéreas e, neste caso, a evapotranspiração é controlada principalmente pela energia disponível (MA et al., 2015; ZHAO et al., 2016).

Por outro lado, a razão  $\lambda E/\lambda E_{eq}$  (PRIESTLEY; TAYLOR, 1972), conhecida como coeficiente de Priestley – Taylor ( $\alpha$ ), é amplamente usada para denotar o controle da evapotranspiração por fatores atmosféricos e fisiológicos, principalmente caracterizando as condições de seca superficial do ecossistema (GENG et al., 2020; KANG et al., 2015; MARQUES et al., 2020). Assim, a  $\lambda E_{eq}$  depende unicamente do saldo de radiação e da

temperatura. Isto demonstra que valores mais baixos ou mais altos indicam que as taxas de evapotranspiração são menores ou maiores do que a taxa de equilíbrio, respectivamente (YAN et al., 2017). Por tanto, uma razão  $\lambda E/\lambda E_{eq} < 1$  representa um ecossistema que sofre limitações no abastecimento de água e, portanto, experimenta reduções na transpiração; quando  $\lambda E/\lambda E_{eq} > 1$ , tem-se um ecossistema úmido, sem limitações de água e apenas a energia disponível limita a evapotranspiração (KANG et al., 2015). O  $\lambda E/\lambda E_{eq}$  é geralmente relacionado ao LAI, ao teor de água do solo e às condições meteorológicas (por exemplo,  $R_n$  e VPD) (GONG et al., 2021; HAO; BAIK; CHOI, 2019; MARQUES et al., 2020; QIU et al., 2019).

### 3 CONSIDERAÇÕES GERAIS

As florestas do Bioma de Mata Atlântica possuem grande importância a nível mundial pela prestação de diferentes serviços ambientais associados à diversidade, assim como à regulação climática e hidrológica. No entanto, é bem conhecida a pressão antrópica que sofrem estes ecossistemas sobre áreas altamente urbanizadas, que constantemente geram mudanças no uso do solo e processos de fragmentação dos ecossistemas. A redução da floresta nativa e sua degradação, interfere nos processos hidrológicos das bacias hidrográficas, afetando a dinâmica no sistema solo-planta-atmosfera no tocante aos processos de evapotranspiração e fluxos de água no solo, principalmente.

Nesse sentido, o foco principal deste estudo foi analisar e modelar os padrões espaço-temporais da evapotranspiração e seus controles biofísicos, bem como os componentes do balanço hídrico: interceptação da chuva pelo dossel, umidade do solo e os diferentes fluxo de água, para compreender a dinâmica hidrológica em um remanescente de Mata Atlântica. Primeiramente, com dados de medições de precipitação (externa e interna), escoamento pelo tronco e umidade no solo em um período de 7 anos hidrológicos (2014 a 2020), foram determinados a interceptação, o armazenamento de água no solo e a evapotranspiração observada em 31 pontos de monitoramento. Posteriormente, com dados de medições meteorológicas realizadas em uma torre de observação, foi modelada a evapotranspiração diária com o modelo de Penman-Monteith (PM) de fonte única. O modelo foi testado por meio da comparação da evapotranspiração observada e simulada. Finalmente, foi calculado o fluxo de água subterrânea abaixo da zona radicular (percolação), apresentando um balanço hídrico anual para o período de estudo.

Dessa forma, com as informações obtidas, foram analisados os padrões hidrológicos das florestas de Mata Atlântica, mostrando sua importância na manutenção dos recursos hídricos. Também foram analisados os processos e variáveis que interferem na evapotranspiração, sendo essenciais para a compreensão dos processos microclimáticos e fisiológicos neste ecossistema. Assim, este trabalho pode ser aplicado como ferramenta na tomada de decisões e aplicações de políticas públicas encaminhadas à preservação dos recursos hídricos e os serviços ecossistêmicos das florestas no Bioma de Mata Atlântica, contribuindo ao suporte científico necessário para sua proteção e manejo adequado.

#### 4 REFERÊNCIAS BIBLIOGRÁFICAS

- ABDOLGHAFORIAN, A. et al. Characterizing the effect of vegetation dynamics on the bulk heat transfer coefficient to improve variational estimation of surface turbulent fluxes. **Journal of Hydrometeorology**, v. 18, n. 2, p. 321–333, 2017.
- ABDOLLAHI, K.; BAZARGAN, A.; MCKAY, G. **Water Balance Models in Environmental Modeling**. Germany: Springer: Berlin, 2019.
- AGUILOS, M. et al. Interannual and seasonal variations in ecosystem transpiration and water use efficiency in a tropical rainforest. **Forests**, v. 10, n. 1, 2019.
- ALLEN, R. G. et al. **Crop evapotranspiration guidelines for computing crop water requirements**. Rome: FAO, 1998.
- ALVARES, C. A. et al. Köppen's climate classification map for Brazil. **Meteorologische Zeitschrift**, v. 22, n. 6, p. 711–728, 2014.
- BORGES, C. K. et al. Seasonal variation of surface radiation and energy balances over two contrasting areas of the seasonally dry tropical forest (Caatinga) in the Brazilian semi-arid. **Environmental Monitoring and Assessment**, v. 192, n. 8, 2020.
- BROEDEL, E. et al. Deep soil water dynamics in an undisturbed primary forest in central Amazonia: Differences between normal years and the 2005 drought. **Hydrological Processes**, v. 31, n. 9, p. 1749–1759, 2017.
- CABRAL, O. M. R. et al. Water and energy fluxes from a woodland savanna (cerrado) in southeast Brazil. **Journal of Hydrology: Regional Studies**, v. 4, n. PB, p. 22–40, 2015.
- CHOUDHURY, B. J.; IDSO, S. B.; REGINATO, R. J. Analysis of an empirical model for soil heat flux under a growing wheat crop for estimating evaporation by an infrared-temperature based energy balance equation. **Agricultural and Forest Meteorology**, v. 39, n. 4, p. 283–297, 1987.
- COELHO, C. A. S.; CARDOSO, D. H. F.; FIRPO, M. A. F. Precipitation diagnostics of an exceptionally dry event in São Paulo, Brazil. **Theoretical and Applied Climatology**, v. 125, n. 3–4, p. 769–784, 2016.
- COSTA, M. H. et al. Atmospheric versus vegetation controls of Amazonian tropical rain forest evapotranspiration: Are the wet and seasonally dry rain forests any different? **Journal of Geophysical Research: Biogeosciences**, v. 115, n. 4, p. 1–9, 2010.
- DA ROCHA, H. R. et al. Seasonality of water and heat fluxes over a tropical forest in eastern Amazonia. **Ecological Applications**, v. 14, n. 4 SUPPL., p. 22–32, 2004.
- DA SILVA, D. A. et al. Drivers of leaf area index variation in Brazilian Subtropical Atlantic Forests. **Forest Ecology and Management**, v. 476, p. 118477, 15 nov. 2020.
- ELLISON, D. et al. Trees, forests and water: Cool insights for a hot world. **Global Environmental Change**, v. 43, p. 51–61, 1 mar. 2017.
- ERSHADI, A. et al. Impact of model structure and parameterization on Penman-Monteith type evaporation models. **Journal of Hydrology**, v. 525, p. 521–535, 1 jun. 2015.

- FELTRIN, R. M. et al. Lysimeter soil water balance evaluation for an experiment developed in the Southern Brazilian Atlantic Forest region. **Hydrological Processes**, v. 25, n. 15, p. 2321–2328, 2011.
- FISCHER, M. et al. Evapotranspiration of a high-density poplar stand in comparison with a reference grass cover in the Czech-Moravian Highlands. **Agricultural and Forest Meteorology**, v. 181, p. 43–60, 2013.
- FORD, C. R.; HUBBARD, R. M.; VOSE, J. M. Quantifying structural and physiological controls on variation in canopy transpiration among planted pine and hardwood species in the southern Appalachians. **Ecohydrology**, v. 130, n. February, p. 126–130, 2010.
- FRAGA, C. I. DE M. et al. Condutância do dossel, condutância aerodinâmica e fator de desacoplamento em floresta de Vochysia divergens Pohl (Vochysiaceae) no Pantanal Brasileiro. **Revista Brasileira de Meteorologia**, v. 30, n. 3, p. 275–284, 2015.
- FREITAS, W. K. DE et al. Tree composition of urban public squares located in the Atlantic Forest of Brazil: A systematic review. **Urban Forestry and Urban Greening**, v. 48, n. September 2019, 2020.
- FRIESEN, J.; LUNDQUIST, J.; VAN STAN, J. T. Evolution of forest precipitation water storage measurement methods. **Hydrological Processes**, v. 29, n. 11, p. 2504–2520, 2015.
- G. PYPKER, T.; S. TARASOFF, C.; KOH, H.-S. Assessing the Efficacy of Two Indirect Methods for Quantifying Canopy Variables Associated with the Interception Loss of Rainfall in Temperate Hardwood Forests. **Open Journal of Modern Hydrology**, v. 02, n. 02, p. 29–40, 2012.
- GENG, J. et al. Dynamics and environmental controls of energy exchange and evapotranspiration in a hilly tea plantation, China. **Agricultural Water Management**, v. 241, n. March, p. 106364, 2020.
- GHIMIRE, C. P. et al. Transpiration and canopy conductance of two contrasting forest types in the Lesser Himalaya of Central Nepal. **Agricultural and Forest Meteorology**, v. 197, p. 76–90, 2014.
- GONG, X. et al. Evapotranspiration partitioning of greenhouse grown tomato using a modified Priestley–Taylor model. **Agricultural Water Management**, v. 247, p. 106709, 31 mar. 2021.
- HAO, Y.; BAIK, J.; CHOI, M. Developing a soil water index-based Priestley–Taylor algorithm for estimating evapotranspiration over East Asia and Australia. **Agricultural and Forest Meteorology**, v. 279, p. 107760, 15 dez. 2019.
- IGARASHI, Y. et al. Environmental control of canopy stomatal conductance in a tropical deciduous forest in northern Thailand. **Agricultural and Forest Meteorology**, v. 202, p. 1–10, 2015.
- IIDA, S. et al. Evapotranspiration from the understory of a tropical dry deciduous forest in Cambodia. **Agricultural and Forest Meteorology**, v. 295, n. September, p. 108170, 2020.
- JARVIS, P. G. The interpretation of the variations in leaf water potential and stomatal conductance found in canopies in the field. **Philosophical Transactions of the Royal Society of London. B, Biological Sciences**, v. 273, n. 927, p. 593–610, 1976.

- JASECHKO, S. et al. Terrestrial water fluxes dominated by transpiration. **Nature**, v. 496, n. 7445, p. 347–350, 2013.
- JASSAL, R. S. et al. Carbon sequestration and water use of a young hybrid poplar plantation in north-central Alberta. **Biomass and Bioenergy**, v. 56, p. 323–333, 1 set. 2013.
- JIAO, L. et al. Determining the independent impact of soil water on forest transpiration: A case study of a black locust plantation in the Loess Plateau, China. **Journal of Hydrology**, v. 572, n. March, p. 671–681, 2019.
- JONES, H. et al. Water balance, surface conductance and water use efficiency of two young hybrid-poplar plantations in Canada's aspen parkland. **Agricultural and Forest Meteorology**, v. 246, n. August 2016, p. 256–271, 2017.
- JUNQUEIRA, J. A. et al. Time-stability of soil water content (SWC) in an Atlantic Forest - Latosol site. **Geoderma**, v. 288, p. 64–78, 2017.
- JUNQUEIRA, J. A. et al. Rainfall partitioning measurement and rainfall interception modelling in a tropical semi-deciduous Atlantic forest remnant. **Agricultural and Forest Meteorology**, v. 275, n. October 2018, p. 170–183, 2019.
- KALMA, J. D.; MCVICAR, T. R.; MCCABE, M. F. Estimating land surface evaporation: A review of methods using remotely sensed surface temperature data. **Surveys in Geophysics**, v. 29, n. 4–5, p. 421–469, 2008.
- KAMALI, M. I. et al. The Determination of Reference Evapotranspiration for Spatial Distribution Mapping Using Geostatistics. **Water Resources Management**, v. 29, n. 11, p. 3929–3940, 2015.
- KANG, M. et al. Energy partitioning and surface resistance of a poplar plantation in northern China. **Biogeosciences**, v. 12, n. 14, p. 4245–4259, 2015.
- KELLIHER, F. M. et al. Maximum conductances for evaporation from global vegetation types. **Agricultural and Forest Meteorology**, v. 73, n. 1–2, p. 1–16, 1995.
- KOOL, D. et al. **A review of approaches for evapotranspiration partitioning** Agricultural and Forest Meteorology Elsevier B.V., , 15 jan. 2014.
- KUME, T. et al. Ten-year evapotranspiration estimates in a Bornean tropical rainforest. **Agricultural and Forest Meteorology**, v. 151, n. 9, p. 1183–1192, 2011.
- LAUNIAINEN, S. et al. Modeling boreal forest evapotranspiration and water balance at stand and catchment scales: a spatial approach. **Hydrology and Earth System Sciences**, v. 23, n. 8, p. 3457–3480, 2019.
- LI, X. et al. A simple and objective method to partition evapotranspiration into transpiration and evaporation at eddy-covariance sites. **Agricultural and Forest Meteorology**, v. 265, n. May 2018, p. 171–182, 2019.
- LI, Z. et al. Evapotranspiration of a tropical rain forest in Xishuangbanna, southwest China. **Hydrological Processes**, v. 24, n. 17, p. 2405–2416, 2010.
- LIU, S. M. et al. Measurements of evapotranspiration from eddy-covariance systems and large aperture scintillometers in the Hai River Basin, China. **Journal of Hydrology**, v. 487, p. 24–

38, 22 abr. 2013.

- LOESCHER, H. W. et al. Energy dynamics and modeled evapotranspiration from a wet tropical forest in Costa Rica. **Journal of Hydrology**, v. 315, n. 1–4, p. 274–294, 2005.
- LU, X. et al. Potential of solar-induced chlorophyll fluorescence to estimate transpiration in a temperate forest. **Agricultural and Forest Meteorology**, v. 252, p. 75–87, 15 abr. 2018.
- MA, N. et al. Environmental and biophysical controls on the evapotranspiration over the highest alpine steppe. **Journal of Hydrology**, v. 529, p. 980–992, 2015.
- MACEDO, T. M. et al. Diversity of growth responses to recent droughts reveals the capacity of Atlantic Forest trees to cope well with current climatic variability. **Forest Ecology and Management**, v. 480, p. 118656, 15 jan. 2021.
- MARKEWITZ, D. et al. Soil moisture depletion under simulated drought in the Amazon: Impacts on deep root uptake. **New Phytologist**, v. 187, n. 3, p. 592–607, 2010.
- MARQUES, T. V. et al. Environmental and biophysical controls of evapotranspiration from Seasonally Dry Tropical Forests (Caatinga) in the Brazilian Semiarid. **Agricultural and Forest Meteorology**, v. 287, n. March, 2020.
- MASEYK, K. et al. Physiology – phenology interactions in a productive semi-arid pine forest. n. C, p. 603–616, 2008.
- MELLO, C. R. et al. Water balance in a neotropical forest catchment of southeastern Brazil. **Catena**, v. 173, n. November 2017, p. 9–21, 2019.
- MELLO, C. R. DE; LIMA, J. M.; SILVA, A. Evapotranspiração em microbacia hidrográfica de fluxo efêmero associada à umidade do solo 1 Evapotranspiration in small ephemeral-watershed associated with soil moisture θ. **Revista Brasileira de Agrometeorologia**, v. 12, n. 1, p. 95–102, 2004.
- MO, X. et al. Simulating temporal and spatial variation of evapotranspiration over the Lushi basin. **Journal of Hydrology**, v. 285, n. 1–4, p. 125–142, 2004.
- MONTEITH, J. L. Evaporation and environment. **Symposia of the Society for Experimental Biology**, n. 19, p. 205–234, 1965.
- MU, Q.; ZHAO, M.; RUNNING, S. W. Improvements to a MODIS global terrestrial evapotranspiration algorithm. **Remote Sensing of Environment**, v. 115, n. 8, p. 1781–1800, 2011.
- MUÑOZ-VILLERS, L. E. et al. Water balances of old-growth and regenerating montane cloud forests in central Veracruz, Mexico. **Journal of Hydrology**, v. 462–463, p. 53–66, 2012.
- MYERS, M. et al. Biodiversity hotspots for conservation priorities. **Nature**, v. 403, n. 2, p. 853–858, 2000.
- NEGRÓN JUÁREZ, R. I. et al. Control of dry season evapotranspiration over the Amazonian forest as inferred from observation at a Southern Amazon forest site. **Journal of Climate**, v. 20, n. 12, p. 2827–2839, 2007.
- NORMAN, J. M.; KUSTAS, W. P.; HUMES, K. S. Source approach for estimating soil and vegetation energy fluxes in observations of directional radiometric surface temperature.

**Agricultural and Forest Meteorology**, v. 77, n. 3–4, p. 263–293, 1995.

OLIVEIRA-FILHO, A. T. et al. **Comparison of the woody flora and soils of six areas of montane semideciduous forest in southern minas gerais, Brazil**. [s.l: s.n.]. v. 51

OLIVEIRA, P. T. et al. Trends in water balance components across the Brazilian Cerrado. **Water Resources Research**, v. 50, n. 9, p. 7100–7114, 2014.

PAKPARVAR, M. et al. Artificial recharge efficiency assessment by soil water balance and modelling approaches in a multi-layered vadose zone in a dry region. **Hydrological Sciences Journal**, v. 63, n. 8, p. 1183–1202, 2018.

PEREIRA, D. et al. Evapotranspiration and estimation of aerodynamic and stomatal conductance in a fragment of Atlantic Forest in Mantiqueira Range Region, MG. **Cerne**, v. 16, p. 32–40, 2010.

POORTER, L. et al. Biomass resilience of Neotropical secondary forests. **Nature**, v. 530, n. 7589, p. 211–214, 2016.

PRIESTLEY, C. H. B.; TAYLOR, R. J. On the Assessment of Surface Heat Flux and Evaporation Using Large-Scale Parameters. **Monthly Weather Review**, v. 100, n. 2, p. 81–92, 1972.

QIU, R. et al. Evapotranspiration estimation using a modified Priestley-Taylor model in a rice-wheat rotation system. **Agricultural Water Management**, v. 224, p. 105755, 1 set. 2019.

REZENDE, C. L. et al. From hotspot to hopespot: An opportunity for the Brazilian Atlantic Forest. **Perspectives in Ecology and Conservation**, v. 16, n. 4, p. 208–214, 1 out. 2018.

RODRIGUES, A. F. et al. Soil water content and net precipitation spatial variability in an Atlantic forest remnant. **Acta Scientiarum - Agronomy**, v. 42, p. 1–13, 2020.

SALEMI, L. F. et al. Land-use change in the Atlantic rainforest region: Consequences for the hydrology of small catchments. **Journal of Hydrology**, v. 499, p. 100–109, 2013.

SANTOS TERRA, M. DE C. N. et al. Stemflow in a neotropical forest remnant: vegetative determinants, spatial distribution and correlation with soil moisture. **Trees - Structure and Function**, v. 32, n. 1, p. 323–335, 2018.

SCARANO, F. R.; CEOTTO, P. Brazilian Atlantic forest: impact, vulnerability, and adaptation to climate change. **Biodiversity and Conservation**, v. 24, n. 9, p. 2319–2331, 2015.

SHEIL, D. Forests, atmospheric water and an uncertain future: the new biology of the global water cycle. **Forest Ecosystems**, v. 5, n. 1, 2018.

SILBERSTEIN, R. P. et al. Modelling the energy balance of a natural jarrah (*Eucalyptus marginata*) forest. **Agricultural and Forest Meteorology**, v. 115, n. 3–4, p. 201–230, 2003.

SU, Z. The Surface Energy Balance System (SEBS) for estimation of turbulent heat fluxes. **Hydrology and Earth System Sciences**, v. 6, n. 1, p. 85–99, 2002.

TABARI, H.; HOSSEINZADEH TALAE, P. Sensitivity of evapotranspiration to climatic change in different climates. **Global and Planetary Change**, v. 115, p. 16–23, 1 abr. 2014.

TAFFARELLO, D. et al. **Hydrological services in the Atlantic Forest, Brazil: An**

**ecosystem-based adaptation using ecohydrological monitoring** Climate Services Elsevier B.V., , 1 dez. 2017.

TAMBOSI, L. R. et al. A framework to optimize biodiversity restoration efforts based on habitat amount and landscape connectivity. **Restoration Ecology**, v. 22, n. 2, p. 169–177, 2014.

TAN, Z. H. et al. Surface conductance for evapotranspiration of tropical forests: Calculations, variations, and controls. **Agricultural and Forest Meteorology**, v. 275, n. June, p. 317–328, 2019.

TOMASELLA, J. et al. The water balance of an Amazonian micro-catchment: the effect of interannual variability of rainfall on hydrological behaviour. **Hydrological Processes**, v. 2274, n. November 2008, p. 2267–2274, 2008.

TOR-NGERN, P. et al. Water balance of pine forests: Synthesis of new and published results. **Agricultural and Forest Meteorology**, v. 259, n. April, p. 107–117, 2018.

VON RANDOW, R. DE C. S. et al. Evapotranspiration and gross primary productivity of secondary vegetation in Amazonia inferred by eddy covariance. **Agricultural and Forest Meteorology**, v. 294, p. 108141, 15 nov. 2020.

YAN, C. et al. Effects of forest evapotranspiration on soil water budget and energy flux partitioning in a subalpine valley of China. **Agricultural and Forest Meteorology**, v. 246, n. June, p. 207–217, 2017.

ZANINI, A. M. et al. The effect of ecological restoration methods on carbon stocks in the Brazilian Atlantic Forest. **Forest Ecology and Management**, v. 481, n. November 2020, p. 118734, 2021.

ZHAO, L. et al. Evapotranspiration estimation methods in hydrological models. **Journal of Geographical Sciences**, v. 23, n. 2, p. 359–369, 2013.

ZHAO, W. et al. Evapotranspiration partitioning, stomatal conductance, and components of the water balance: A special case of a desert ecosystem in China. **Journal of Hydrology**, v. 538, p. 374–386, 2016.

ZHENG, H. et al. Spatial variation in annual actual evapotranspiration of terrestrial ecosystems in China: Results from eddy covariance measurements. **Journal of Geographical Sciences**, v. 26, n. 10, p. 1391–1411, 2016.

## **SEGUNDA PARTE – ARTIGO**

### **EVAPOTRANSPIRATION AND WATER BALANCE IN A NEOTROPICAL FOREST OF SOUTHEASTERN BRAZIL**

#### **ABSTRACT**

The Atlantic Forest ecosystems have a highly relevance due to numerous ecosystem services provided by them. It is understood by UNESCO as one of the most important biosphere reserves in the world. However, these ecosystems have been threatened by anthropogenic pressures. The aim of this study was to evaluate the evapotranspiration and the water balance components in a remaining fragment of the Atlantic Forest (AFR) based on hydrometeorological datasets from seven hydrological years (2014-2020). The main focus was to analyze and to model the spatial and temporal patterns of evapotranspiration and their biophysical controls as well as the water balance components of the canopy rainfall interception, soil moisture and the different pathways of the water. On average, the rainfall canopy interception was significant account for 19% of total gross precipitation (P), whereas evapotranspiration accounted for an average of 77% of P. The processes involved with evapotranspiration is controlled by stomatal and soil water storage, mainly in the dry periods. Based on the water balance analyzes, the water that flows below the root zone (DP) showed a variation between 3% and 49% of P. Therefore, despite the water limitations during the analyzed period, the Neotropical forest stands out as a key element to provide ecological functions, mainly for controlling and storage water.

**Keywords:** soil water storage, biophysical controls, rainfall interception, space-time analysis

## 1 INTRODUCTION

The Atlantic Forest Biome is the home to more than 60% of Brazil's urban population and has suffered different degrees of pressure in recent centuries. This situation causes losses of vegetation, fragmentation of forests, and, consequently, impacts on the climate and hydrological regimes (SCARANO; CEOTTO, 2015; ZANINI et al., 2021). Taffarello et al. (2017) and Macedo et al. (2021) highlighted the importance of Atlantic Forests as providers of water services, mitigating persistent droughts, and reduction natural hazards that hit these areas in Brazil. UNESCO has recognized the Atlantic Forest as one of the most important biosphere reserves worldwide due to its high diversity and endemism, as well as its environmental relevance (MYERS et al., 2000). Currently, the biome has only 28% of its original coverage, in which 91% have passed through continuous fragmentation processes. In addition, 46% of the remnants are under a strong edge effect (MACEDO et al., 2021; POORTER et al., 2016) and have low resilience capacity (TAMBOSI et al., 2014). These facts show the urge for preservation of the remaining biodiversity and ecohydrological functions (DA SILVA et al., 2020; REZENDE et al., 2018). To support strategies that lead to Atlantic Forest conservation and its rational use, it is relevant to study the hydrological dynamics and processes involved in this ecosystem. Since evapotranspiration (E) plays a critical role in the connection with water and energy cycles (CABRAL et al., 2015; COSTA et al., 2010; MARQUES et al., 2020; TAN et al., 2019), its accurate evaluation and influence on the water balance of the Atlantic Forests is a key element for a better understanding of the regional climate dynamics, water yield and quality, and to improve the management of these ecosystems.

Although several studies have focused on the evapotranspiration of Atlantic Forest biomes (MELLO et al., 2019; PEREIRA et al., 2010; SALEMİ et al., 2013), they are mainly short-term studies, spanning less than two years of evaluation. Hydrology in some areas of the Atlantic Forest is affected by a marked seasonality of the climate (dry winters and wet summers), granting its semi-deciduous nature (FREITAS et al., 2020). Most species of semi-deciduous ecosystems generally self-regulate the physiological process of transpiration, losing their foliage in rainless periods to avoid water stress (MARQUES et al., 2020). This behavior should be considered in studies of the forest water balance, as it can affect the water storage capacity throughout the year (MELLO et al., 2019). Therefore, the abovementioned studies offered partial insights into the dynamics of evapotranspiration and water pathways in this ecosystem.

In Atlantic Forest areas, detailed knowledge regarding the space-time variability of evapotranspiration, the influence of interactive meteorological variables, vegetation composition, phenology, and soil water attributes are still lacking, as well as the energy partitioning in the ecosystem and the biophysical controls of evapotranspiration. On the other hand, studies carried out in this type of forests have not portrayed extreme climatic events, e.g., droughts and heavy rainfalls to evaluate the changes in the annual patterns of water and energy balance. Therefore, further knowledge on evapotranspiration and the partitioning of the water balance on the Atlantic Forest ecosystem based on long-term hydrometeorological measurements is needed.

Such studies have been carried out in other ecosystems in Brazil through direct measurements of evapotranspiration flux, using the Eddy Covariance system (e.g., DA ROCHA et al., 2004; CABRAL et al., 2015; MARQUES et al., 2020). However, there are effective methodologies for indirectly calculating evapotranspiration, such as energy and water balance with residual focus (JONES et al., 2017). Thus, evapotranspiration models, like the large leaf or Penman-Monteith (PM), validated against real measurements, are capable of capturing the variability of climate and soil water storage, making the water balance analyzes reliable in forests ecosystems (JONES et al., 2017; KUME et al., 2011; PEREIRA et al., 2010).

In this context, this study aims to evaluate the evapotranspiration and the components of the water balance of an Atlantic Forest remnant (AFR), based on hydrometeorological information spanning seven hydrological years (2014-2020). In this context, we sought to: (i) identify the dynamics of the rainfall interception, its partitioning, and the influences on soil water storage; (ii) evaluate the space-time pattern of evapotranspiration based on hydrological information and identify its main drivers; (iii) estimate the annual elements of the water balance of the AFR during the study period.

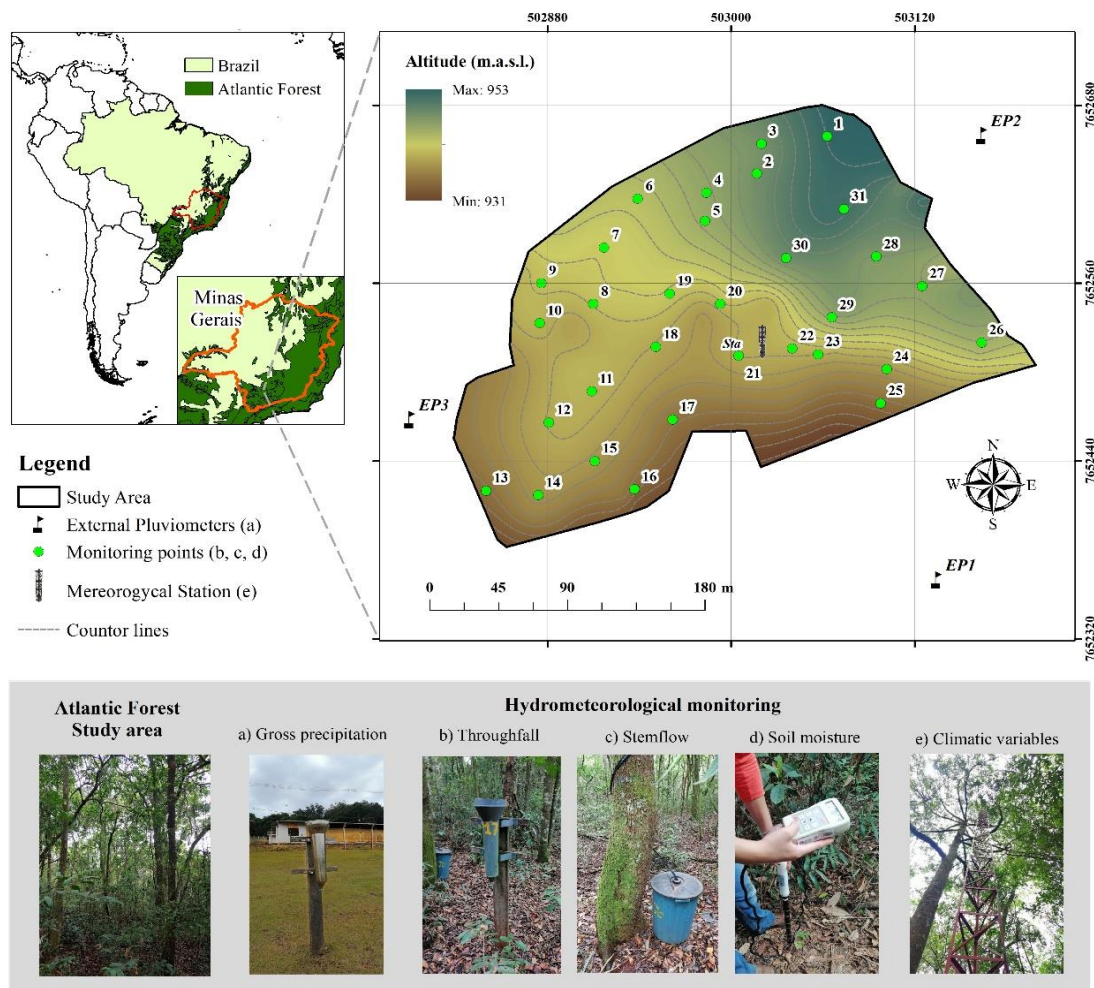
## 2 MATERIAL AND METHODS

### 2.1 Site description

The studied area (Figure 1) is located in Southeast Brazil, in the coordinates 21°13'40"S and 44°57'50"W, with an average altitude of 925 meters above mean sea level (m.a.s.l.). Consists in a remnant of a Mountain Seasonal Semideciduous Forest (MSSF) with 6.35 ha. The soil is characterized as Oxisols (USDA Soil Taxonomy), which is distributed over a slightly undulated relief with declivities < 15% (JUNQUEIRA et al., 2017). According to the Köppen

climate classification, the region's climate is a mesothermal subtropical type, i.e. Cwa, with well-defined precipitation seasonality (ALVARES et al., 2014), with two periods: wet (between October and March) and dry (between April and September). According to Junqueira et al. (2019), the annual average precipitation is 1461.8 mm, with 84% concentrated in the wet season. The annual average temperature is 20.3 °C, varying from 16.9 °C in July to 22.8 °C in February. The annual average humidity is 73.1%, varying from 62.3% in August to 79.8% in December and January.

Figure 1 - Geographical location and instrumentation used for hydrometeorological monitoring elements in the Atlantic Forest experimental area, in southeastern Brazil.



Source: The Author (2020).

The experimental area is periodically monitored in terms of vegetation parameters (forest inventory) since 1994, in which are measured the changes on species growing, mortality, and other dendrometric variables. At first, it was inventoried 6,527 individuals by Oliveira-Filho et al. (1994), however, it was registered 5609 ones in the last forest inventory (2017).

Such individuals are represented by 48 botanical families and 184 species. The most representative families are: Annonaceae (830), Fabaceae (769), Lauraceae (720), Rubiaceae (671), Myrtaceae (510), Meliaceae (431), and Melastomataceae (363). The most frequent species are: *Xylopia brasiliensis* (670), *Copaifera langsdorffii* (517), *Amaioua intermedia* (497), *Trichilia emarginata* (383), *Miconia willdenowii* (282), *Myrcia splendens* (262), and *Casearia arborea* (195).

The forest is in a stage of transition (Kozlowski, 2002) with 87.68% of individuals in minor classes of diameter at breast height (DBH), being represented between 5-15 cm (68.41%) and 15-25 cm (19.29%). The other classes correspond to 12.32%, in which the 25-35 cm class comprehends 8.34% and that greater than 35 cm, 3.97%. The forest canopy average height is 10.2 m with a few dispersed individuals higher than 20 m (JUNQUEIRA et al., 2019). The canopy stratification has four levels: (i) a layer of emerging trees (>20 m) dispersed in the studied area; (ii) a layer of the main canopy (10-15 m); (iii) a layer of shrub and young trees (<10 m); and (iv) an herbal cover over the soil. There are openings in the canopy caused by fallen and dead trees that have completed their cycle, which modify the species' dynamic and the remnant's structure.

## 2.2 Water balance monitoring

Gross precipitation (P), i.e., the incoming precipitation, was measured between October 2013 and September 2020. In this period, 644 rainy events were monitored. At first, between 2013 and 2017, the measurement was carried out through two procedures: (i) automatic monitoring, performed every hour using an 8-inch tipping-bucket rain gauge that covers 324.3 cm<sup>2</sup> (TE525-L, Texas Electronics Inc., Dallas, TX, EUA); and (ii) daily manual monitoring, performed using a totalizing-type “Ville de Paris” rain gauge with a collected area of 378.5 cm<sup>2</sup>. Both rain gauges were installed at a 22 m high Micrometeorological Observation Tower (MOT), located in near the center of the studied area (Figure 1). From August 2017, other three totalizing-type rain gauges were installed surrounding the AFR to improve the spatial representativeness of P (Figure 1a).

Thirty-one points were randomly selected inside the AFR to measure throughfall (TF), stemflow (Stf), and soil moisture ( $\theta$ ) up to 1.0 m depth. These points are on average spaced for 40 m from each other. TF measurement (Figure 1b) was carried out with a “Ville de Paris” rain gauge installed 1.5 m above the forest floor to avoid splash-in (JUNQUEIRA et al., 2019). To guarantee that the canopy has completely drained and to avoid bias, data collection was performed four hours after the rainfall had ceased.

Stf was measured in one representative tree (Figure 1c) for each monitoring point. The individuals were selected according to localization, abundance, and dominant species (TERRA et al., 2018). The collectors were constructed with polyethylene hose set in the tree trunks in a spiral scheme, applying silicone between the collector and tree to avoid leaking (PYPKER; TARASOFF; KOH, 2012). The stemflow was drained into a container and collected at the same time as TF.

In each monitoring point, permanent access tubes were installed (Figure 1d), approximately every 15 days, to measure the soil moisture ( $\text{m}^3\text{m}^{-3}$ ) in five depths (0.10 m, 0.20 m, 0.30 m, 0.40 m, and 1.0 m). The measurement was carried out with a multi-sensor capacitance probe (model PR2/6, Delta-T Devices Ltd.).

Since forest evapotranspiration relies on soil water availability, we calculated the relative extractable water (REW) (Allen et al. 1998):

$$\text{REW} = \frac{(\theta - \theta_{wp})}{(\theta_{fc} - \theta_{wp})} \quad (1)$$

where  $\theta$ ,  $\theta_{fc}$ , and  $\theta_{wp}$ , are the water volumetric content, the field capacity, and the wilting point, that were obtained by Rodrigues et al. (2020) in the AFR.

### 2.3 Meteorological and LAI measurements

In the MOT (Figure 1e), micrometeorological sensors were installed in two heights, being one at the top of the forest canopy (22 m high) and another at 2 m above ground. Each level contains sensors for relative humidity (RH) and temperature ( $T_a$ ) measurements (Model S-THB-M002). A pyranometer set (measuring incoming and outgoing radiation) (Model S-LIB-M003) for net radiation ( $R_n$ ), a barometric pressure sensor (Model CS100), and an anemometer (Model 03002) for wind speed and direction were also installed. The sensor data were hourly stored in a CR10x programmable data-logger (Campbell Scientific, Logan, UT, USA).

The leaf area index (LAI in  $\text{m}^2 \text{m}^{-2}$ ) was measured monthly in the last hydrological year (2019-2020) at the 31 monitoring points, using a previously calibrated and validate Sun Scan zeptometer system (Model SS1-STD3, Delta-T Devices Ltd., Cambridge, UK). These LAI datasets were used to parametrization the heat flux from the soil considered in the Penman-Monteith model for evapotranspiration estimates in AFR.

## 2.4 Elements for water balance calculation

The water balance of a forest remnant was computed according to Jones et al., (2017):

$$\frac{DP}{\Delta T} = \frac{P - E - \Delta S}{\Delta T} \quad (2)$$

where P (mm) is the gross precipitation, E (mm) is the evapotranspiration,  $\Delta S$  (mm) is the variation in soil water storage (SWS) integrated over the root zone (1.0 m in this study), DP (mm) is the deep water percolation leaving the root zone and  $\Delta T$  is the interval adopted for the water balance (monthly). Jones et al. (2017) stated that in this equation the values of the runoff were disregarded due to their low influence on the water balance under a forest ecosystem. P was calculated by averaging the precipitation of the external rain gauges to the forest.  $\Delta S$  was calculated, for each set of monitoring, as the monthly difference of the SWS, being a function of the soil moisture readings. Although tropical forests can uptake water from deeper layers during drought conditions (MARKEWITZ et al., 2010), this amount is of minor contribution in total evapotranspiration as it is restricted to short periods (BROEDEL et al., 2017). Thus, the root water uptake was considered up to 1.0 m depth, since we observed a decrease in fine roots abundance during the installation of the moisture tubes. SWS was calculated as follows:

$$SWS = \sum_{i=1}^n \left( \frac{\theta_i + \theta_{i+1}}{2} \times h \right) \quad (3)$$

$$\frac{\Delta S}{\Delta T} = \frac{SWS_{(j+t)} - SWS_{(t)}}{\Delta T} \quad (4)$$

where  $\theta_i$  e  $\theta_{i+1}$  are, respectively, soil moisture at depth i and  $i + 1 (m^3 m^{-3})$ , n is the number of layers (0–0.10 m; 0.1–0.2 m; 0.20 –0.30 m; 0.30–0.40 m; 0.40–1.0 m), h is the thickness of each layer (mm), j is the water balance time step and t is the consecutive date of each measurement.

However, monitoring DP in thirty-one points for each rainfall event is laborious and time-consuming. In this regard, the evapotranspiration (E) can be calculated by means of a water balance (EWB) in periods of low rainfall, when percolation can be neglected. EWB was determined based on Tomasella et al. (2008) and Mello et al. (2019), taking the observed rainfall events that only recharge up to 1.0 m depth. As a result, the equation for EWB can be rewritten:

$$\frac{E_{(WB)}}{\Delta T} = \frac{(TF + Stf) - \Delta S_{(0-1.0\text{ m})} + C}{\Delta T} \quad (5)$$

where C is the canopy rainfall interception (mm), obtained through the equation described by Ghimire et al. (2014) and Junqueira et al. (2019):

$$\frac{C}{\Delta T} = \frac{P - (TF + Stf)}{\Delta T} \quad (6)$$

DP was estimated as a residue of the water balance from Eq.2. According to Jones et al. (2017), this simplification implies that in situations when P exceeds E, DP is positive, which means that the water is leaving the root zone, i.e., percolation. On the other hand, when E exceeds P, DP is negative, and water is entering the root zone (capillary rise).

## 2.5 Parameterization of the evapotranspiration model and components

Due to the lack of data measured for DP, the water balance in the wet season (October-March) was run calculating evapotranspiration modeled using the Penman - Monteith  $E_{(PM)}$  model. It was also performed through a parameterization of the  $E_{(PM)}$  with simple evaporative source, which encompasses soil evaporation, evaporation of intercepted water and plant transpiration into a single evaporative element (ERSHADI et al., 2015), which is used to describe the physiological and environmental conditions (MONTEITH, 1965; KELLIHER et al., 1995). The version is expressed as:

$$E_{(PM)} = \frac{\Delta \cdot (R_n - G) + \rho_a \cdot c_p \cdot g_a \cdot (VPD)}{\lambda \cdot \left[ (\Delta + \gamma) \cdot \left( 1 + \frac{g_a}{g_s} \right) \right]} \quad (7)$$

which  $E_{(PM)}$  is the modeled real evapotranspiration to the ecosystem ( $\text{mm d}^{-1}$ );  $\lambda$  is the latent heat of water vaporization ( $\text{MJ kg}^{-1}$ );  $\Delta$  is the declivity of saturation vapor pressure curve ( $\text{kPa}^{\circ}\text{C}^{-1}$ );  $R_n$  is the net radiation ( $\text{MJ m}^{-2} \text{d}^{-1}$ );  $G$  is the heat flux in the soil ( $\text{MJ m}^{-2} \text{d}^{-1}$ );  $\gamma$  is the psychrometric coefficient ( $\text{kPa}^{\circ}\text{C}^{-1}$ );  $\rho_a$  is the air density ( $\text{kg m}^{-3}$ ); VPD is the water vapor pressure deficit ( $\text{kPa}$ ) (APÊNDICE A – Variáveis complementares do modelo PM;  $C_p$  is the specific heat at a constant pressure ( $\text{J kg}^{-1}^{\circ}\text{C}^{-1}$ ) (approximately  $1,000 \text{ J kg}^{-1}^{\circ}\text{C}^{-1}$ );  $g_a$  is the aerodynamic conductance ( $\text{m s}^{-1}$ ), and  $g_s$  is the canopy conductance ( $\text{m s}^{-1}$ ).

In this research,  $G$  was obtained through the empirical model of Choudhury et al. (1987) that relates LAI with  $R_n$  as  $G = 0.079 \cdot [\exp(-0.24 \cdot \text{LAI})] \cdot R_n$ . Given that  $G$  is very small in forest ecosystems (ALLEN et al., 1998) and the lack of LAI monitoring for the entire period, the values of the monitoring carried out in 2019-2020 were considered.

The aerodynamic conductance ( $g_a$ ) was determined by focusing on Monin-Obukhov (GARRAT; HICKS, 1973; LOESCHER et al., 2005) theory, which is based on vertical wind profile. Such a modeling was daily performed; the measurement was restricted to neutral conditions of balance in the atmosphere according to Allen et al. (1998):

$$g_a = \frac{k^2 \cdot u(z)}{\left\{ \ln \left[ \frac{(z-d)}{z_{OM}} \right] \right\}^2} \quad (8)$$

Being  $u$  the wind speed ( $m s^{-1}$ ) in the  $z$  measurement high (m) (at the height of 22 m),  $d$  is the zero-plane displacement (m),  $z_{OM}$  is surface roughness (m), and  $k$  is the von Kármán constant (0.41). Values of  $z_{OM}$  and  $d$  considered in this Atlantic rainforest were  $(0.1) \cdot h_c$  e  $(2/3) \cdot h_c$ , respectively;  $h_c$  corresponds to canopy average high, approximately 10.2 m.

There is a major difficulty in the canopy conductance parameterization and several models with empirical approach that link various parameters that influence in gases exchange in the stomata have been proposed (TAN et al., 2019). In this study,  $g_s$  was obtained by the Penman-Monteith (Eq. 7) equation, using indirect values of  $\lambda E$  extracted from the energy balance with residual focus (FISCHER et al., 2013; SU, 2002):

$$R_n - G - H = \lambda E_{res}. \quad (9)$$

This involves the measurement of sensible heat flux  $H$  ( $MJ m^{-2} d^{-1}$ ) using the "Inversing Bulk Transfer Equation" method (based on Monin-Obukhov similarity theory, MOST) (NORMAN; KUSTAS; HUMES, 1995). That method has been applied in different research with micrometeorological approach and remote sensors for the evaluation of energy flux (KALMA; MCVICAR; MCCABE, 2008; SILBERSTEIN et al., 2003), being  $H$  expressed as:

$$H = c_p \cdot \rho_a \cdot g_a \cdot (T_1 - T_2) \quad (10)$$

where  $T_1$  is the air temperature near an aerodynamic surface at canopy height ( $^{\circ}C$ );  $T_2$  is the air temperature near surface ( $^{\circ}C$ ).  $T_1$  is the temperature measured on the meteorological tower (22.0 m height) while  $T_2$  was measured inside the AFR, 2.0 m above forest floor. The analysis was made considering average daily temperatures over the two levels.

To support the knowledge of the physical controls of evapotranspiration in AFR, the decoupling coefficient ( $\Omega$ ) and Priestley-Taylor coefficient ( $\alpha$ ) were calculated. Thus, the evapotranspiration sensitivity to changes in canopy characteristics and local atmosphere conditions can be evaluated through the  $\Omega$  (MCNAUGHTON; JARVIS, 1983):

$$\Omega = \frac{1}{1 + \left[ \frac{\gamma}{(\Delta + \gamma)} \right] \cdot \left[ \frac{g_a}{g_s} \right]} \quad (11)$$

According to Ma et al. (2015) and Marques et al. (2020),  $\Omega$  varies from 0 to 1. Values close to 0 indicate that evapotranspiration is mostly controlled by stomata closure, whereas values close to 1 indicate that energy balance is the limiting factor of evapotranspiration.

Furthermore, to assess whether either atmospheric demand or soil moisture supply was also controlling evapotranspiration,  $\alpha$  was calculated (PRIESTLEY; TAYLOR, 1972). This is equivalent to the ratio between evapotranspiration and the equilibrium evapotranspiration ( $E_{eq}$ ) (depends on net radiation and temperature):

$$\alpha = \frac{\lambda E}{\lambda E_{eq}} = \frac{\lambda E}{\left[ \frac{(R_n - G) \Delta}{(\Delta + Y)} \right]} \quad (12)$$

where  $\lambda E$  is the modeled latent heat flux (Eq. 9).  $R_n$ ,  $G$ ,  $\Delta$  and  $\gamma$  were described previously. Values of  $\alpha < 1$ , denote limitations of the ecosystem to the water supply; and  $\alpha > 1$  represents a humid ecosystem, i.e., there are no water limitations and only the available energy limits evapotranspiration (MARQUES et al., 2020).

## 2.6 Spatial modeling and precision statistics

The spatial modeling was performed to identify spatial patterns of evapotranspiration in the AFR taking as reference the dry season (from April to September) of each hydrological year between 2014 and 2020. The spatial variability was evaluated through geostatistical procedures (ordinary kriging method) and the coefficient of variation (CV) among 31 sampled points of the water balance (Figure 1). The interpolations were performed in ArcGIS (version 10.8) using the exponential semivariogram model, which is widely used for hydrological and soil physical attributes mapping (JUNQUEIRA et al., 2017; KAMALI et al., 2015; RODRIGUES et al., 2020).

A comparative analysis was performed between modeled evapotranspiration (EPM) and evapotranspiration (EWB) obtained from water balance during months that did not present significant precipitation. Slope hypothesis (line 1:1) and its respective coefficient of determination ( $R^2$ ) were evaluated. The performance of EPM to simulate evapotranspiration in the AFR was evaluated by Root Mean Square Error (RMSE) and Nash-Sutcliffe (NS) coefficient:

$$\text{RMSE} = \sqrt{\frac{1}{N} \left\{ \sum_{i=1}^N (P_i - O_i)^2 \right\}} \quad (13)$$

$$\text{NS} = 1 - \frac{\sum_{i=1}^N (P_i - O_i)^2}{\sum_{i=1}^N (O_i - O_m)^2} \quad (14)$$

where  $P_i$  and  $O_i$  are simulated and observed evapotranspiration at time  $i$ , respectively;  $N$  is the number of simulated and observed pair values; and  $O_m$  is the observed average values. Values of RMSE close to zero mean a good fit, as well as NS values close to 1.

The quality of the spatial interpolations was evaluated by the degree of dependence (DP) and cross-validation, using the reduced mean error (RME) and reduced error standard deviation (RESD):

$$\text{SD} = \frac{C_1}{C_1 + C_0} \quad (15)$$

$$\text{RME} = \frac{1}{N} \sum_{i=1}^N \left( \frac{z(x_i) - z^*(x_i)}{\sigma(x_i)} \right) \quad (16)$$

$$\text{RESD} = \sqrt{\frac{1}{N} \left\{ \sum_{i=1}^N \left( \frac{z(x_i) - z^*(x_i)}{\sigma(x_i)} \right)^2 \right\}} \quad (17)$$

where  $C_0$  is the nugget effect; and  $C_1$  is the sill;  $N$  is the number of local information on cross-validation;  $z(x_i)$  is the observed value at the point  $i$ ;  $z^*(x_i)$  is the simulated value at the point  $i$ ;  $\sigma_i$  is the kriging standard deviation in the  $i$  point. SD classifies the degree of spatial structure, as strong (higher than 75%), moderate (between 25 and 75%) and weak (less than 25%) (CAMBARDELLA et al., 1994). The values RME and RESD close to 0 and 1, respectively, mean a good fitting.

Linear and non-linear regressions were performed to analyze possible relationships between variables of water balance and evapotranspiration, evaluating the regressions with the model's coefficients that were not significant at 5% probability level ( $p < 0.05$ ).

### 3 RESULTS

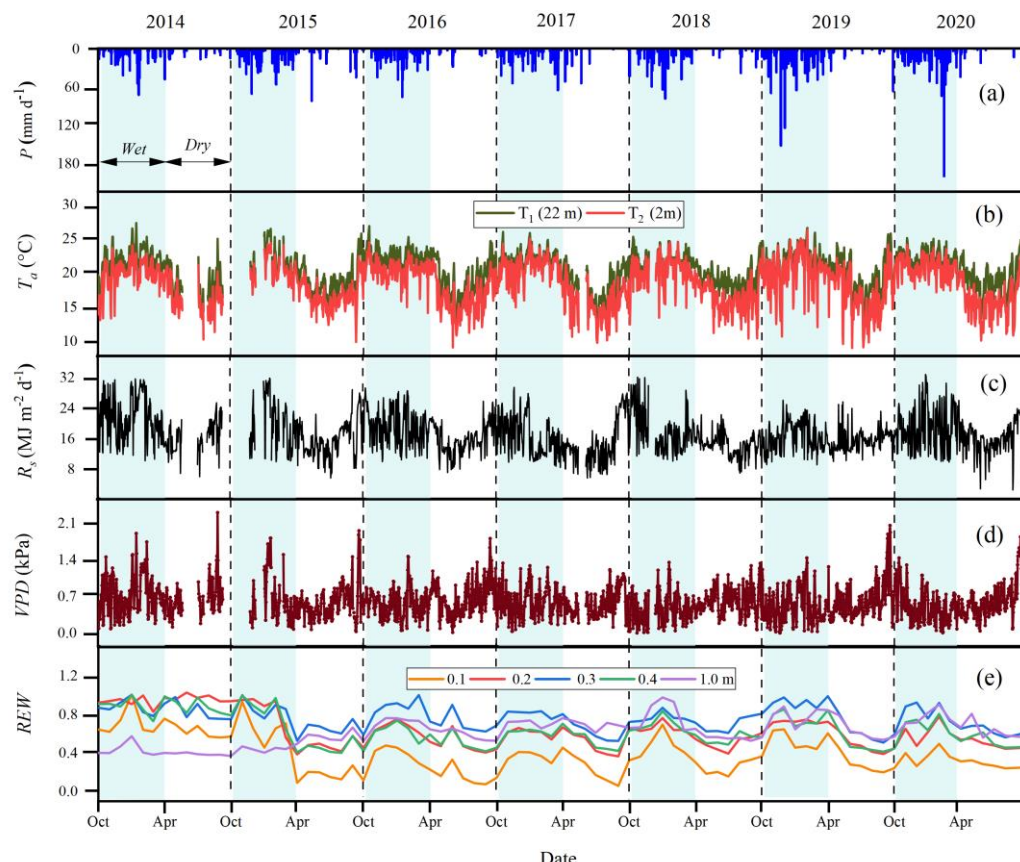
#### 3.1 Meteorological conditions observed in the studied period

During the studied years, the average daily gross precipitation ( $P$ ) at the studied area was  $3.11 \text{ mm d}^{-1}$ , presenting strong seasonal variations (Figure 2a) with the highest values in

the wet season. It presented two events of  $P > 100 \text{ mm d}^{-1}$  in 2018 (November and December) and just one in 2020 (February). The average air temperature ( $T_a$ ) over the forest canopy (Figure 2b) was  $21.85^\circ\text{C}$  in the wet season and  $18.51^\circ\text{C}$  in the dry season, approximately  $0.05^\circ\text{C}$  lower and  $2.51^\circ\text{C}$  higher than long-term average, respectively. Inside the AFR,  $T_a$  varied from  $21.85^\circ\text{C}$  in the wet season to  $15.85^\circ\text{C}$  in the dry season.  $R_s$  (Figure 2c) presents daily seasonal variation with higher radiation intensity in the wet season ( $18.47 \text{ MJ m}^{-2}$ ), and lower values in the dry season ( $15.15 \text{ MJ m}^{-2}$ ). The vapor pressure deficit (VPD) was  $0.58 \text{ kPa}$  and  $0.54 \text{ kPa}$  in the dry and wet season, respectively (Figure 2d).

The relative extractable water (REW) in the five soil depths ( $0.1 \text{ m}$ ,  $0.2 \text{ m}$ ,  $0.3 \text{ m}$ ,  $0.4 \text{ m}$  and  $1.0 \text{ m}$ ) are presented in Figure 2e. During the wet season, REW remained at values close to 1 in all depths, due to frequent rainfalls that fulfill the field capacity. In the dry season, due to water uptake by the forest, REW gradually decreased, mainly in depths of  $0.1$ ,  $0.2$  and  $0.3$ , achieving average values of  $0.24$ ,  $0.44$  and  $0.48$ , respectively.

Figure 2 - Average daily (a) gross precipitation ( $P$ ), (b) daily mean air temperature ( $T_a$ ), (c) daily global solar radiation ( $R_s$ ), (d) deficit of vapor pressure deficit (VPD), and (e) relative extractable water (REW) in the  $0\text{--}1.0\text{m}$  soil layer. Shaded columns represent periods of wet seasons.

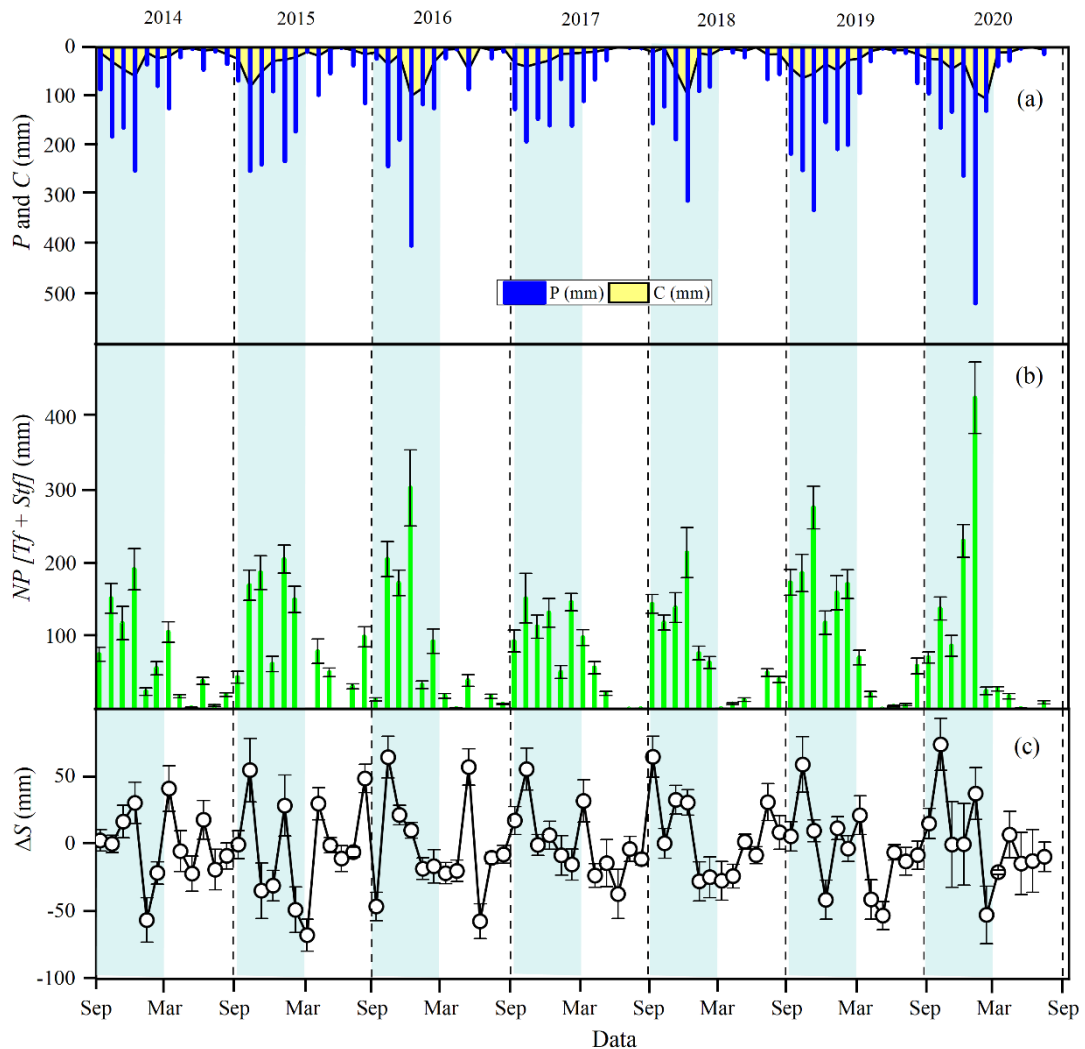


Source: The Author (2020).

### 3.2 Precipitation partitioning and soil water storage behavior in the studied period

The gross precipitation values (Figure 3a) in each hydrological year were 1024 mm (2013-2014), 1350.1 mm (2014-2015), 1229.5 mm (2015-2016), 1043.5 mm (2016-2017), 1087.4 mm (2017-2018), 1561.5 mm (2018-2019), and 1399.8 mm (2019-2020). It was possible to observe that during the study period, most of the years had observed values lower than the long-term average (1461.8 mm), which characterized a prolonged dry period. The daily average values of the year are presented on Table 1.

Figure 3 - Monthly gross precipitation (P) and canopy rainfall interception (C) (a), monthly effective (or net) precipitation (NP), with respective standard deviations (vertical bars) (b), monthly soil water storage variation in the 0-1.0 m control layer ( $\Delta S$ ), with respective standard deviations (vertical bars) (c). Shaded columns represent periods of wet seasons.



Source: The Author (2020).

C had a proportional variation related to the amount of rain in the studied years, resulting in an average of 19.13%. In the hydrological year of 2019-2020, C was 25.3% due to greater rainfall amount, mostly concentrated in 2020. The effective rainfall (rainfall that hits forest floor) represents 81.22% of P, from which TF corresponded to 99.9% of net precipitation (NP). TF ranged from 765.4 mm (2015-2016) to 1239.2 mm (2018-2019). Its annual average in the wet season was 670 mm and in the dry season was 149.6 mm, being 82.06% and 75.21% of P, respectively. The annual average Stf was 2.6 mm and 0.4 mm in wet and dry seasons, which represents 0.1% of P, respectively.

Table 1 - Daily average of gross precipitation (P, mm d<sup>-1</sup>), throughfall (TF, mm d<sup>-1</sup>), streamflow (Stf, mm d<sup>-1</sup>) and canopy rainfall interception in the dry and wet periods of the hydrological years from 2014 to 2020.

Hydrological Year		P	TF	Stf	C
2013-2014	Wet	4.13 ± 2.7	3.19 ± 2.1	0.01 ± 0.02	0.85 ± 0.6
	Dry	0.9 ± 1.5	0.62 ± 1.3	0.01 ± 0.01	0.18 ± 0.2
	Annual	2.51 ± 2.1	1.9 ± 1.7	0.01 ± 0.01	0.52 ± 0.4
2014-2015	Wet	6.67 ± 2.6	5.3 ± 2.2	0.02 ± 0.02	0.87 ± 0.8
	Dry	1.49 ± 1.5	1.34 ± 1.4	0.01 ± 0.01	0.24 ± 0.2
	Annual	4.08 ± 2.1	3.32 ± 1.8	0.01 ± 0.01	0.56 ± 0.5
2015-2016	Wet	5.16 ± 4.3	4.41 ± 3.7	0.01 ± 0.02	1.08 ± 1.2
	Dry	0.51 ± 1.0	0.4 ± 0.51	0.01 ± 0.01	0.13 ± 0.6
	Annual	2.84 ± 2.7	2.4 ± 2.1	0.01 ± 0.01	0.61 ± 0.9
2016-2017	Wet	5.05 ± 1.4	4.07 ± 1.3	0.01 ± 0.01	0.98 ± 0.4
	Dry	0.46 ± 1.5	0.36 ± 1.3	0.01 ± 0.00	0.12 ± 0.1
	Annual	2.76 ± 1.5	2.21 ± 1.3	0.01 ± 0.00	0.54 ± 0.3
2017-2018	Wet	4.54 ± 2.8	4.28 ± 1.8	0.01 ± 0.01	0.45 ± 1.2
	Dry	0.51 ± 0.9	0.33 ± 0.7	0.01 ± 0.00	0.18 ± 0.2
	Annual	2.53 ± 1.9	2.3 ± 1.3	0.01 ± 0.00	0.31 ± 0.7
2018-2019	Wet	7.01 ± 2.0	5.73 ± 1.7	0.01 ± 0.01	1.47 ± 0.4
	Dry	0.66 ± 1.2	0.43 ± 1.0	0.01 ± 0.00	0.23 ± 0.2
	Annual	3.83 ± 1.6	3.08 ± 1.4	0.01 ± 0.00	0.85 ± 0.3
2019-2020	Wet	4.86 ± 5.3	3.73 ± 4.9	0.01 ± 0.02	1.20 ± 1.2
	Dry	0.68 ± 0.5	0.44 ± 0.4	0.01 ± 0.01	0.21 ± 0.1
	Annual	2.77 ± 2.9	2.08 ± 2.6	0.01 ± 0.01	0.72 ± 0.7

Source: The Author (2020).

The seasonality of soil water storage variation ( $\Delta S$ ) stands out with a marked predominance of positive values in the wet season (Figure 3c), with an average value of 28 mm. However, the hydrological years of 2013-2014 and 2014-2015 presented values of -28.5 and -32.2 mm, mainly in 2014. In the dry season, the lack of rainfall presents a higher recession of

soil water storage by water consumption in the ecosystem, averaging -41.4 mm in the studied period.

### 3.3 Modeling and spatiotemporal patterns of evapotranspiration

The daily average evapotranspiration values from water balance performed during the dry season in the studied period (April – September, from 2014 to 2020) are presented in Table 2. Fluctuations of evapotranspiration were observed, varying from 0.90 to 1.75 mm d<sup>-1</sup>, where the hydrological years 2017-2018 and 2014-2015 presented minimum and maximum values, respectively. The CV varied from 5% (2014-2015) to 14.17% (2019-2020), presenting a small variability among the 31 studied sets of monitoring.

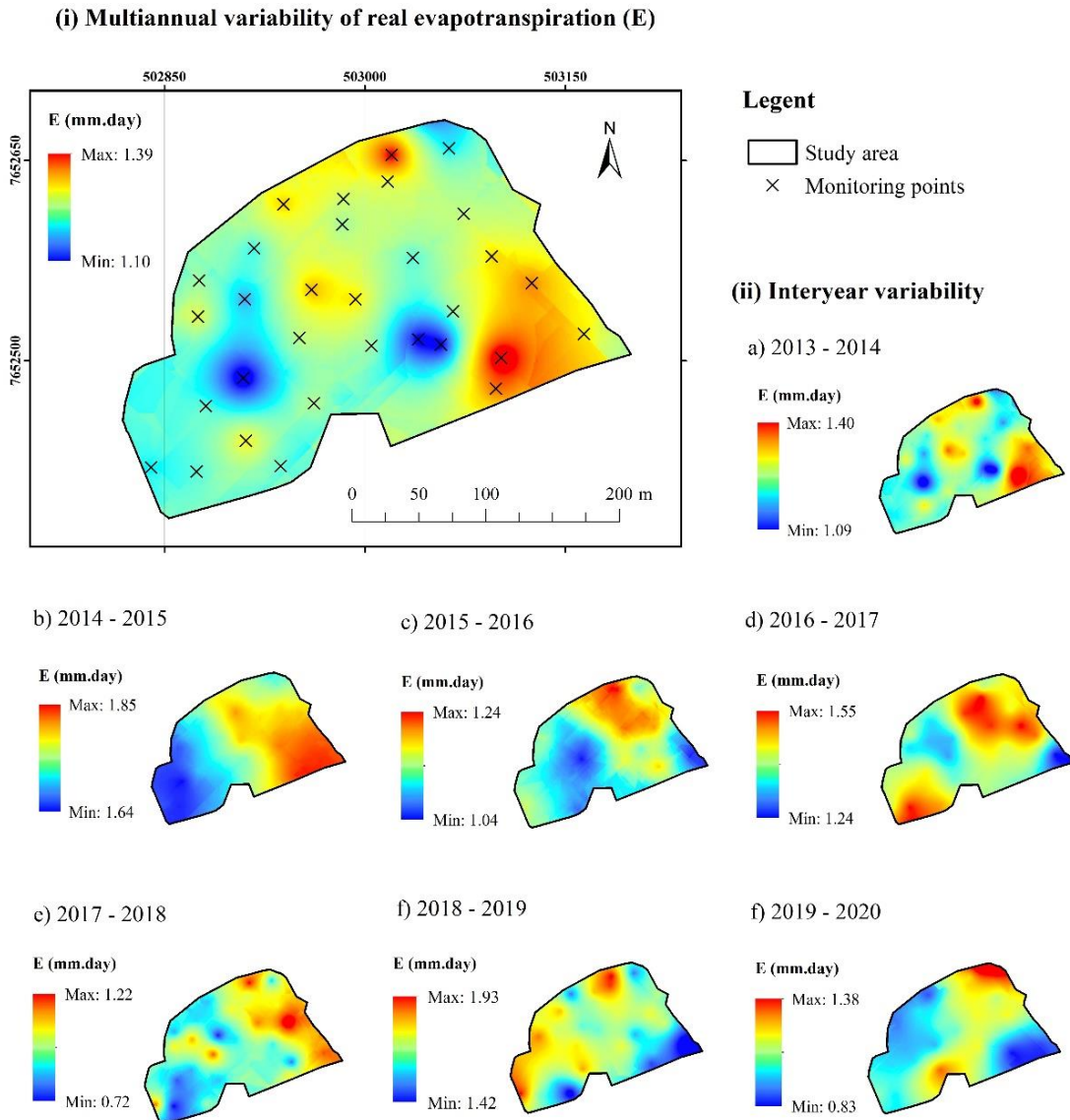
Table 2 - Daily average evapotranspiration of the dry periods (E<sub>WB</sub>, mm d<sup>-1</sup>), the coefficient of variation (CV, %) between the points of the water balance, and precision statistics of the semivariogram model fitted.

Hydrological Year	E	CV (%)	SD (%)	RME	RESD
2013-2014	1.24 ± 0.06	5.18	56.84	-0.010	0.96
2014-2015	1.75 ± 0.08	5.00	52.41	0.007	0.98
2015-2016	1.12 ± 0.08	7.66	61.32	0.009	1.00
2016-2017	1.42 ± 0.08	6.14	47.05	0.027	1.00
2017-2018	0.90 ± 0.10	12.07	99.71	-0.037	1.06
2018-2019	1.72 ± 0.09	5.68	69.26	0.032	0.98
2019-2020	0.99 ± 0.14	14.17	83.62	0.031	0.94
Average	1.25 ± 0.06	4.72	72.91	-0.008	0.95

Source: The Author (2020).

In Figure 4, it is presented the spatial patterns of evapotranspiration in multiannual and annual scales. It can be seen that evapotranspiration does not present a spatial variability pattern within the evaluated years. Also, in Table 2, it is presented the spatial structure degree (SD) of the fitted geostatistical model and the cross-validation statistical precision. A good fitting of the exponential model can be observed. All the years presented moderate to strong spatial structure degrees and RME and RESD values close to 0 and 1, respectively. However, the drier years showed less spatial structure degree of evapotranspiration in AFR.

Figure 4 - Spatial patterns of daily average evapotranspiration in the dry period: (i) multiannual variability (average from 2014 to 2020); (ii) interannual variability.



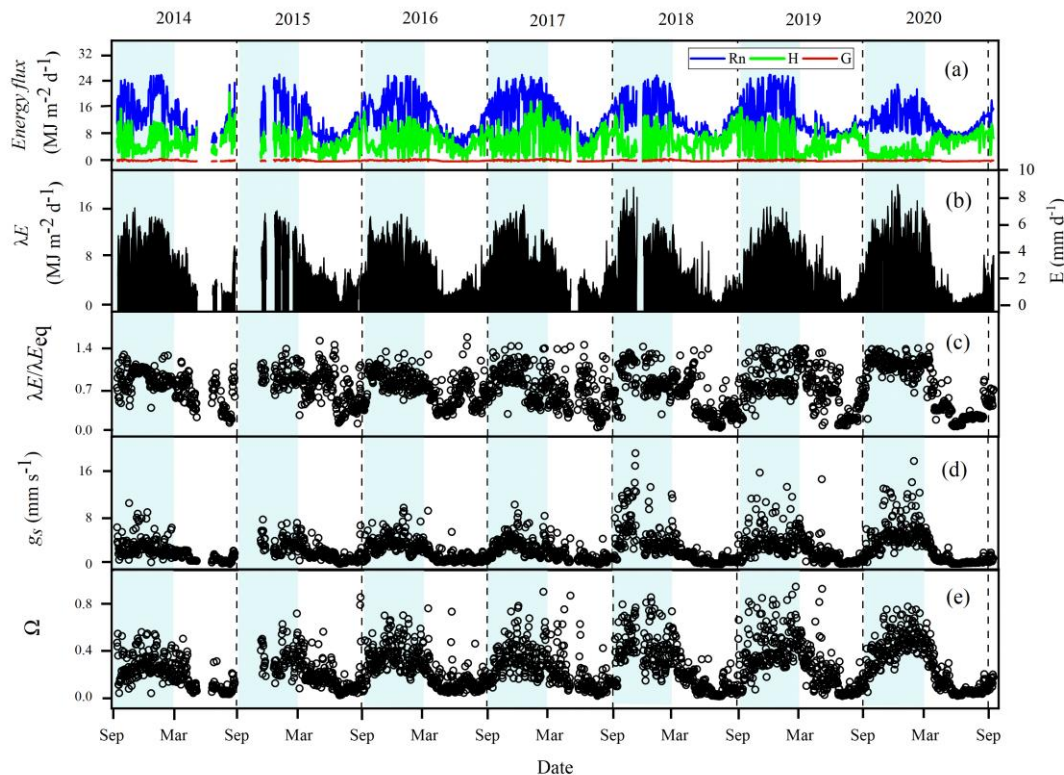
Source: The Author (2020).

The spatial distribution of the modeled daily values of evapotranspiration, energy fluxes, Priestley-Taylor coefficient ( $\alpha$ ), canopy conductance ( $g_s$ ), and the decoupling factor ( $\Omega$ ) are displayed in Figure 5. The  $R_n$  values showed a seasonality average values in the wet season, varying from  $16.21 \text{ MJ m}^{-2} \text{ d}^{-1}$  to  $9.21 \text{ MJ m}^{-2} \text{ d}^{-1}$  in the dry season (Figure 5a). The value of the heat flux in the soil is near zero and does not show a marked variation in the studied period, corresponding on average to  $0.43 \text{ MJ m}^{-2} \text{ d}^{-1}$  in wet seasons and  $0.18 \text{ MJ m}^{-2} \text{ d}^{-1}$  in dry seasons.  $H$  presents a higher seasonality fluctuation in the dry season, with the daily average value of  $6.16 \text{ MJ m}^{-2} \text{ d}^{-1}$ , whereas in the wet season, this value is  $5.37 \text{ MJ m}^{-2} \text{ d}^{-1}$ . On the other hand,

higher values of  $\lambda E$  (Figure 5b) occur in the wet season, with an average value of  $10.28 \text{ MJ m}^{-2} \text{ d}^{-1}$  (equivalent to  $4.20 \text{ mm d}^{-1}$ ), for which it was obtained  $3.11 \text{ MJ m}^{-2} \text{ d}^{-1}$  (equivalent to  $1.27 \text{ mm d}^{-1}$ ).

In terms of  $R_n$ ,  $\lambda E$  corresponds to 60% in the study period. The Priestley-Taylor coefficient ( $\alpha$ ) presented values  $> 1$  in the wet period, indicating that evapotranspiration is controlled by atmospheric demand (Figure 5c) in this period. In the dry periods, an average value of 0.51 indicates that the evapotranspiration is mainly controlled by soil moisture. On the other hand,  $g_s$  (Figure 5d) presented the same seasonal pattern as evapotranspiration with an average value in the wet season of  $3.47 \text{ mm s}^{-1}$  and in the dry season,  $0.85 \text{ mm s}^{-1}$ . Seasonal pattern of  $\Omega$  (Figure 5e) was similar to  $g_s$ . The low values indicate a strong control of evapotranspiration through  $g_s$  in both dry (0.35) and wet (0.10) seasons. In Table 3, it is detailed the daily average values for these components throughout the seven studied hydrological years.

Figure 5 - Annual modeled data of (a) daily energy flux: net radiation, sensible heat flux and soil heat flux ( $R_n$ ,  $H$  and  $G$ ; left scale); (b) latent heat flux ( $\lambda E$ , left scale) and equivalent evapotranspiration in millimeters ( $E$ , right scale); (c) daily coefficient of Priestley-Taylor ( $\alpha = \lambda E / \lambda E_{eq}$ , left scale); (d) daily canopy conductance ( $g_s$ , left scale); and (e) daily decoupling factor ( $\Omega$ , left scale). Shaded columns represent periods of wet seasons.



Source: The Author (2020).

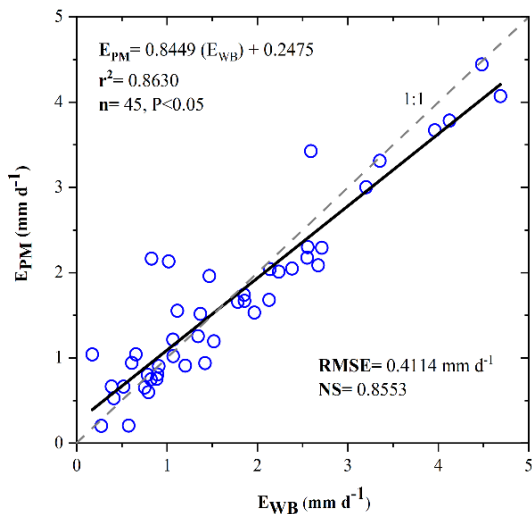
Table 3 - Daily average values of net radiation ( $R_n$ , MJ m $^{-2}$  d $^{-1}$ ), latent heat flux (LE, MJ m $^{-2}$  d $^{-1}$ ), sensible heat flux (H, MJ m $^{-2}$  d $^{-1}$ ), soil heat flux (G, MJ m $^{-2}$  d $^{-1}$ ), latent heat flux ( $\lambda E_{res}$ , MJ m $^{-2}$  d $^{-1}$ ), coefficient of Priestley-Taylor ( $\alpha = \lambda E / \lambda E_{eq}$ ), canopy conductance ( $g_s$ , mm s $^{-1}$ ), decoupling factor ( $\Omega$ ) and evapotranspiration (E, mm d $^{-1}$ ) in the dry, wet and annual time scales of the hydrological years from 2014 to 2020.

Hydrological Year		$R_n$	H	G	$\lambda E_{res}$	A	$g_s$	$\Omega$	E
2013-2014	Wet	15.89 ± 5.1	5.38 ± 3.1	0.45 ± 0.2	10.64 ± 2.9	0.89 ± 0.2	2.29 ± 1.6	0.25 ± 0.1	4.33 ± 1.2
	Dry	9.44 ± 3.3	5.62 ± 3.1	0.2 ± 0.1	3.26 ± 2.2	0.57 ± 0.3	0.69 ± 0.7	0.09 ± 0.1	1.33 ± 0.9
	Anual	12.67 ± 4.2	5.5 ± 3.1	0.32 ± 0.1	6.95 ± 2.5	0.73 ± 0.2	1.49 ± 1.2	0.17 ± 0.1	2.83 ± 1.0
2014-2015	Wet	17.48 ± 5.9	6.09 ± 3	0.47 ± 0.2	10.49 ± 3.4	0.9 ± 0.2	3.39 ± 1.5	0.31 ± 0.1	4.29 ± 1.4
	Dry	8.61 ± 3.8	4.95 ± 3.2	0.17 ± 0.1	4.3 ± 1.60	0.63 ± 0.3	1.34 ± 1	0.14 ± 0.1	1.75 ± 0.7
	Anual	13.04 ± 4.9	5.52 ± 3.1	0.32 ± 0.1	7.39 ± 2.5	0.77 ± 0.2	2.36 ± 1.2	0.22 ± 0.1	3.02 ± 1.0
2015-2016	Wet	16.95 ± 4.7	5.6 ± 3.1	0.42 ± 0.2	10.05 ± 2.3	0.86 ± 0.2	3.34 ± 1.5	0.33 ± 0.1	4.1 ± 0.90
	Dry	8.87 ± 3.8	6.26 ± 2.6	0.17 ± 0.1	2.82 ± 2.1	0.55 ± 0.2	0.88 ± 0.6	0.11 ± 0.1	1.15 ± 0.8
	Anual	12.91 ± 4.3	5.93 ± 2.8	0.29 ± 0.1	6.43 ± 2.2	0.7 ± 0.2	2.11 ± 1.1	0.22 ± 0.1	2.63 ± 0.9
2016-2017	Wet	18.71 ± 5.1	7.06 ± 4.2	0.45 ± 0.2	9.63 ± 3.0	0.87 ± 0.3	3.17 ± 1.6	0.31 ± 0.1	3.93 ± 1.3
	Dry	10.1 ± 3.9	7.24 ± 3.2	0.19 ± 0.1	3.44 ± 2.1	0.57 ± 0.3	1.04 ± 1.0	0.12 ± 0.1	1.4 ± 0.8
	Anual	14.4 ± 4.5	7.15 ± 3.7	0.32 ± 0.1	6.53 ± 2.6	0.72 ± 0.3	2.11 ± 1.3	0.22 ± 0.1	2.67 ± 1.0
2017-2018	Wet	15.56 ± 4.7	5.53 ± 3.6	0.45 ± 0.2	10.42 ± 3.3	0.84 ± 0.2	3.75 ± 3.7	0.41 ± 0.2	4.26 ± 1.4
	Dry	9.08 ± 3.2	6.51 ± 3.1	0.17 ± 0.1	2.29 ± 2.0	0.33 ± 0.3	0.6 ± 0.7	0.07 ± 0.1	0.94 ± 0.8
	Anual	12.32 ± 3.9	6.02 ± 3.4	0.31 ± 0.1	6.36 ± 2.7	0.59 ± 0.3	2.18 ± 2.2	0.24 ± 0.1	2.6 ± 1.10
2018-2019	Wet	15.82 ± 5.9	5.76 ± 4.3	0.4 ± 0.2	10.1 ± 3.0	0.81 ± 0.3	3.62 ± 2.4	0.38 ± 0.2	4.13 ± 1.3
	Dry	9.07 ± 1.5	5.33 ± 2.3	0.18 ± 0.1	3.78 ± 2.3	0.62 ± 0.3	0.91 ± 1.1	0.12 ± 0.1	1.54 ± 0.9
	Anual	12.45 ± 3.7	5.54 ± 3.3	0.29 ± 0.1	6.94 ± 2.6	0.71 ± 0.3	2.27 ± 1.7	0.25 ± 0.2	2.83 ± 1.1
2019-2020	Wet	13.1 ± 3.5	2.2 ± 1.3	0.34 ± 0.1	10.66 ± 3.1	1.15 ± 0.1	4.71 ± 2.7	0.45 ± 0.1	4.35 ± 1.3
	Dry	9.36 ± 2.7	7.22 ± 1.7	0.18 ± 0.1	1.91 ± 1.9	0.27 ± 0.2	0.48 ± 0.6	0.06 ± 0.1	0.78 ± 0.8
	Anual	11.23 ± 3.1	4.71 ± 1.5	0.26 ± 0.1	6.29 ± 2.5	0.71 ± 0.2	2.59 ± 1.6	0.25 ± 0.1	2.57 ± 1.0

Source: The Author (2020).

The evapotranspiration model fitted in this study is supported by the meteorological data and estimated canopy conductance. It was capable of adequately estimating the actual evapotranspiration to the AFR. In Figure 6, the relationship between EPM (Penman-Monteith evapotranspiration) and EWB (water balance evapotranspiration) can be highlighted. The regression line is not significantly different from line 1:1, indicating the accuracy of the modeled evapotranspiration. Moreover, the values of Root Mean Square Error (RMSE) were 0.4114 mm d $^{-1}$ , and the Nash–Sutcliffe (NS) coefficient 0.8553, meaning that the modeled evapotranspiration were close to those calculated from water balance.

Figure 6 - Relationship between modeled evapotranspiration ( $E_{PM}$ ) and evapotranspiration from water balance ( $E_{WB}$ ) and precision statistics (RMSE e NS).



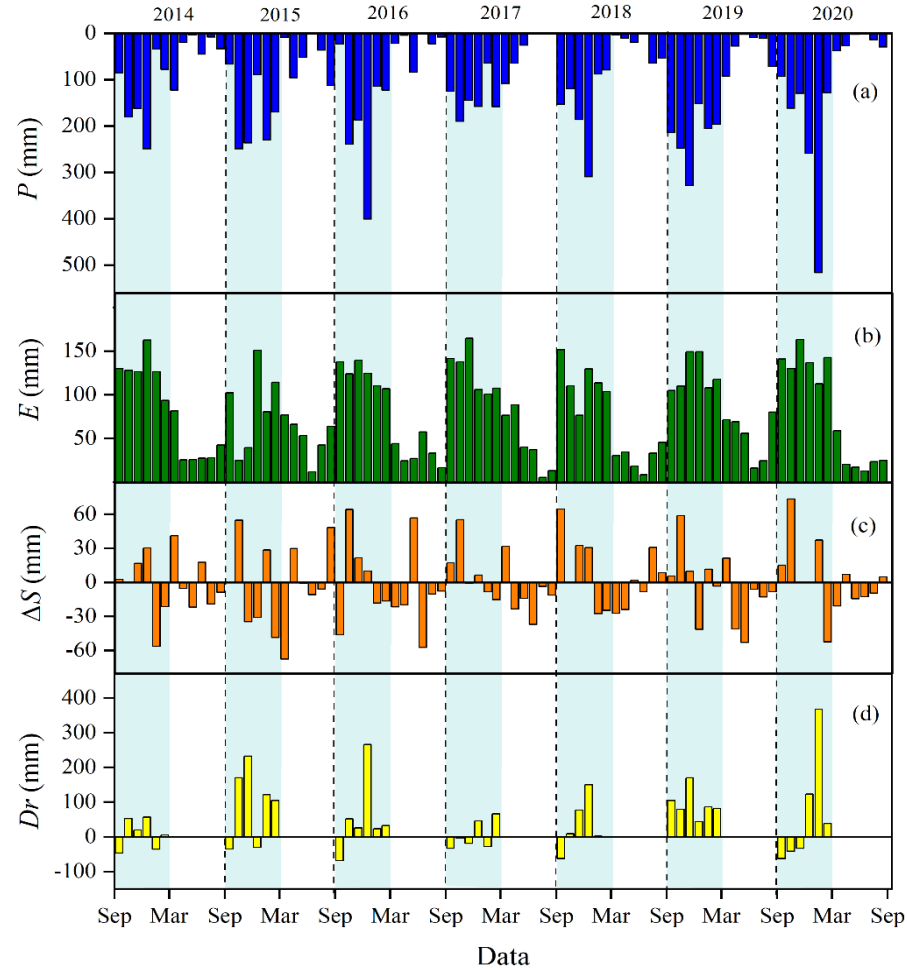
Source: The Author (2020).

### 3.4 Water balance elements

Figure 7 presents the components of the monthly water balance in AFR. During the studied period, the maximum values of P and E were observed in 2018-2019 hydrological year, being 1561.5 and 1055.8 mm, respectively. It can be noted that E monthly behavior followed the seasonal pattern of P. However, in very rainy months (such as February 2020), E behavior tends to be differentiated, due to the influence of radiation. The monthly  $\Delta S$  was predominantly positive in wet periods and negative in dry periods (Figure 7c). Annually, it stands out with positive values in 2016-2017, 2017-2018, and 2019-2020.

From the analysis of the modeled evapotranspiration, it was possible to estimate the percolation (DP) for periods with significant rainfall. On an annual scale, DP is predominantly positive with an average value of 323.76 mm in the study period. In years characterized by drier conditions (2013-2014, 2016-2017, and 2017-2018), it was observed a decrease of the annual DP regarding to the wetter years (Figure 7d).  $E_{PM}$  showed a marked participation in the drier years, which affected the percolation, mainly in the months of September (after the dry period) and February (with higher atmospheric demand).

Figure 7 - Monthly water balance components: (a) Gross precipitation (P); (b) evapotranspiration (EPM); (c) water storage variation ( $\Delta S$ ) in root zone; and (d) the water percolation (DP) for the seven hydrological studied years (2014 to 2020).



Source: The Author (2020).

## 4 DISCUSSION

### 4.1 Precipitation partitioning and soil water storage behavior

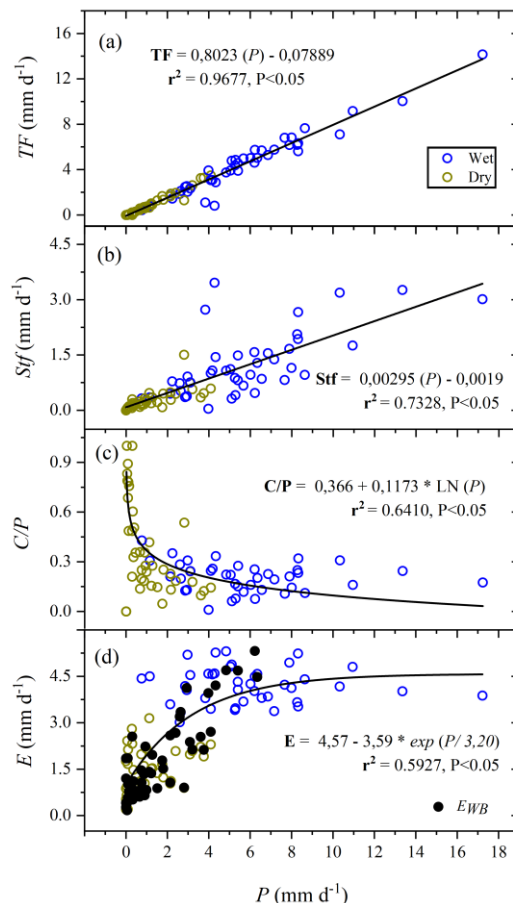
Seasonal patterns of the precipitation within AFR follow the behavior of the regional precipitation pattern, which is characterized by a wet season (summer) and a dry season (winter). In the last decade, the Brazilian southeast region presented a significant decrease in precipitation regarding the long-term average value. The hydrological years of 2013-2014, 2016-2017, and 2017-2018 were characterized by severe droughts all over the southeast, mainly in the wet season (COELHO; CARDOSO; FIRPO, 2016; JUNQUEIRA et al., 2019).

TF (Figure 8a) and Sft (Figure 8b) followed the seasonal pattern of P, i.e., presents a direct relationship. On the other hand, the relationship between C and P varies because of the

differences in the ecosystem as a response to their structure and diversity. For instance, Mello et al. (2019) found a C/P ratio of 20.9% for an Atlantic Rainforest at Mantiqueira Mountain Range, in southeastern Brazil. Salemi et al. (2013) found up to 33% for this ratio in a neotropical forest at Serra do Mar Mountain Range, also in southeastern Brazil. Iida et al. (2020) observed values of 5.3% in a deciduous dry rainforest in Kratie, Camboja. Such differences are related to the foliage size and roughness of species. In the AFR, C/P has a decreasing logarithmic relationship with P (Figure 8c), demonstrating that the smaller the rainfall amount the greater the interception.

An exponential relationship between evapotranspiration and P is highlighted in Figure 8d. Evapotranspiration increases with P as a consequence of a higher water availability that provides stomata opening and gas exchange during photosynthesis. This behavior can be observed when analyzing the differences in the evapotranspiration of the wet (blue dots) and dry periods (green dots). A stabilization is reached for great amounts of precipitation from which the water availability is no longer the limiting factor for evapotranspiration.

Figure 8 - Relationships between average observed gross rainfall (P): (a) throughfall (TF); (b) stemflow; (c) C/P ratio (Stf); and (d) real evapotranspiration (E).



Source: The Author (2020).

Seasonality of  $\Delta S$  (0-1.0m) follows P variations showing that the AFR is sensitive to small changes in rainfall pattern. In this way, prolonged drought conditions can potentially create major deficits of water in the soil, including in months of the wet season. Thus, the water storage in the one-meter-depth layer did not have a well-defined seasonal pattern, since January 2016 and February 2020 had low  $\Delta S$  values if compared to the drier months. Junqueira et al. (2017) studied the temporal stability of the soil moisture in the AFR using data from 2012 to 2015. They observed that the forest influences on the time-stability of the soil moisture in shallower depths (up to 0.40 m), while the soil attributes, such as soil saturated hydraulic conductivity, drive the moisture behavior in deeper layers. Mello et al. (2019) found similar results in a forest with the same characteristics but with a shallow soil (Inceptisols). This demonstrates that Atlantic Forests play a crucial role in the temporal and spatial behavior of the soil moisture, impacting in the water balance behavior.

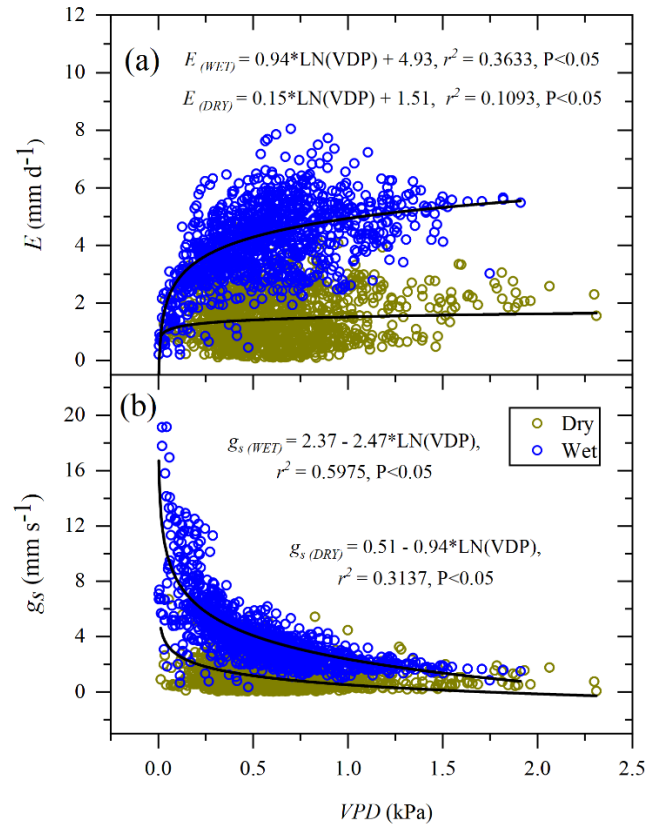
#### **4.2 Modeling and spatiotemporal patterns of evapotranspiration**

Evapotranspiration values obtained in this study are in agreement with Pereira et al. (2010), Salemi et al. (2013), and Mello et al. (2019), all developed in Atlantic Forest ecosystem. They presented daily average values of evapotranspiration of 3.9, 3.56- and 3.26-mm  $d^{-1}$ , respectively. In this study, daily evapotranspiration varies from 4.96 mm  $d^{-1}$  in wet season to 1.55 mm  $d^{-1}$  in dry season. Studies carried out by means eddy covariance and Bowen ratio method in other Brazilian ecosystems (Da Rocha et al. 2004; Marques et al. 2020; Fraga et al. 2015; Cabral et al. 2015) presented daily average values, respectively, of 3.51 mm  $d^{-1}$  (Amazon forest), 1.3 mm  $d^{-1}$  (Caatinga ecosystem), 3.90 mm  $d^{-1}$  (Pantanal ecosystem), and 3.36 mm  $d^{-1}$  (Cerrado ecosystem).

The spatial variability of evapotranspiration is expressive among different types of forest, however, it is poorly studied in tropical forests. To assess it, most of the studies have been based on the coefficient of variation (LAUNIAINEN et al., 2019; MO et al., 2004; ZHENG et al., 2016), in wide spatial scales that impair the analysis of different ecosystems, especially those that are very fragmented. In this study, CV was lower than 14% for all the hydrological years, in which the lowest one was observed in years with stronger droughts. In addition, in these years, it was observed a greater spatial dependence degree obtained by the fitted semivariogram model. This spatial continuity can be associated with the spatial distribution and variability of the water inputs, highlighting soil moisture and heterogeneity of the canopy, both characterized by Rodrigues et al. (2020) for the AFR.

The application of the evapotranspiration model satisfactorily reproduced the observed evapotranspiration from water balance, showing an error of 13.7%, which is consistent with Mello et al. (2019), Muñoz-Villers et al. (2012) and Pereira et al. (2010). This modeling allowed analyzing the seasonal changes in the evapotranspiration in the forest throughout seven hydrological years as they are explained principally by the changes in radiation and soil moisture. In terms of radiation, the percentage of  $R_n$  responded by 60% of the evapotranspiration. This value is in accordance with other studies carried out to Neotropical forests obtained in Brazil and Mexico, which both present semi-deciduous forest sites (CABRAL et al., 2015; DA ROCHA et al., 2004; MUÑOZ-VILLERS et al., 2012).

Figure 9 - Relationships between vapor pressure deficit (VPD) with (a) daily modeled evapotranspiration and (b) daily  $g_s$ .

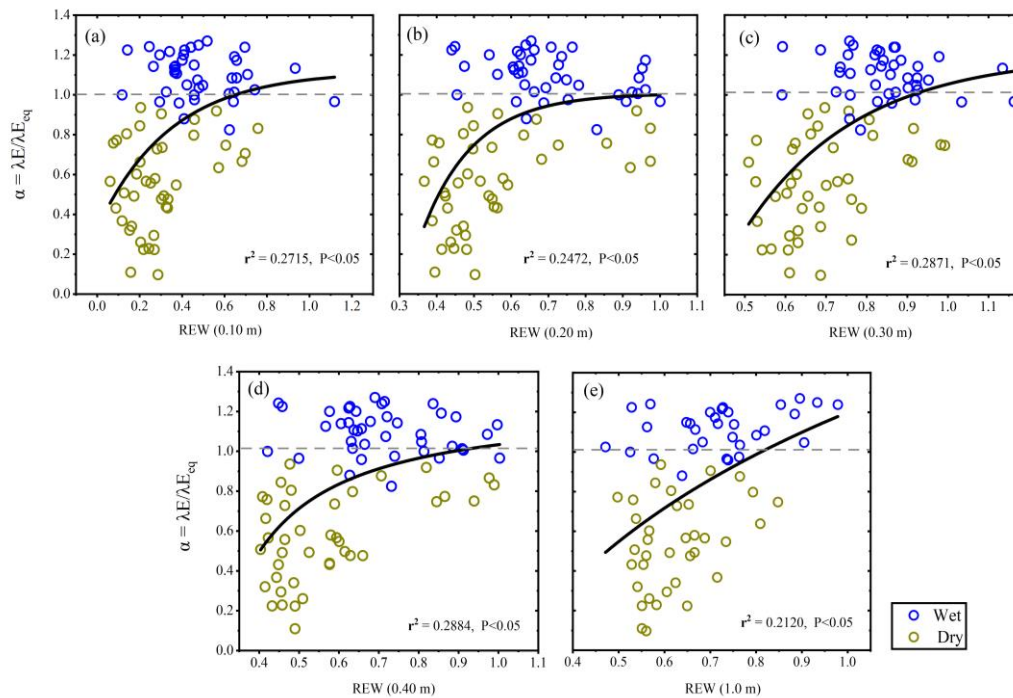


Source: The Author (2020).

The canopy conductance ( $g_s$ ) in the study period presented values according to secondary tropical forests with average daily values ranging from  $0.9 \text{ mm s}^{-1}$  to  $12.7 \text{ mm s}^{-1}$  (CABRAL et al., 2015; DA ROCHA et al., 2004; FRAGA et al., 2015; MARQUES et al., 2020). According Tan et al. (2019), the gas exchange (photosynthesis and transpiration) in tropical forests with marked variation in precipitation decreases during the dry season, as a

forest's strategy to control water and energy losses. This pattern can be seen in the present study, where a reduction of canopy conductance is observed between March and September (dry period). Evapotranspiration increases exponentially with changes in the vapor pressure deficit (VPD), more strongly when higher than 0.7 kPa (Figure 9a); however, the gas exchange decreases in the wet period (Figure 9b), showing a stomatal regulation due to the environmental conditions. Cabral et al. (2015) and Igarashi et al. (2015) reported that high values of evapotranspiration occurred before the lowest values of VPD (in rainy periods) because of the increase in stomata opening in response to the water vapor transport gradient.

Figure 10 - Relationships between the monthly mean values of the Priestley-Taylor coefficient ( $\alpha = \lambda E / \lambda E_{eq}$ ) and the relative extractable soil water content (REW) (a. 0.10 m; b. 0.20 m; c. 0.30 m; d. 0.40 m; and e. 1.0 m).



Source: The Author (2020).

In terms of biophysical evapotranspiration controls, the seasonal variations of  $\Omega$  and  $\alpha$  ( $\lambda E / \lambda E_{eq}$ ) were higher in the rainy period of the seven years evaluated, being similar to regions with prolonged dry season (MA et al., 2015; TAN et al., 2019). In general, the results suggest that in AFR, evapotranspiration was mainly driven by stomatal control throughout the period. The distribution of  $\alpha$  showed that in wet periods there is a greater atmospheric demand than in dry periods, which influences stomatal opening due to water availability. This fact can be evidenced in relation to  $\alpha$  with the relative content of extractable water from soil (REW) for five depths from 0.10 to 1.0 m (Figure 10). The behavior in different layers of the soil showed

that the depletion of water is faster in shallower layers (0-0.2 m) since there is greater demand for water by the plants. Maseyk et al. (2008), Aguilos et al. (2019) and Jiao et al. (2019) mentioned that E is strongly limited by soil moisture when water deficits occur, where a drier soil causes a reduction in canopy conductance aiming to avoid water stress during water depletion. This fact is quite important in ecosystems such as the Atlantic Forest, which is under seasonal climate variation with a period with a reduction on precipitation. Therefore, longer drought periods due to likely climate change can affect the water availability in the soil and, thus, on evapotranspiration and photosynthesis processes.

### **4.3 Water balance**

The water balance elements presented important differences throughout the seven hydrological years. On annual scale, the variability of DP (percolation beyond root system) showed that the capillary effect was irrelevant, even in severely dry conditions. However, in months where E exceeded P, DP becomes negative. This occurs mainly in months after the dry period, where evapotranspiration tends to increase due to changes in radiation (begging the spring and summer). Therefore, small changes in rainfall can contribute to reduce the water percolation in this ecosystem. In addition, our results, like other studies (e.g., LI et al., 2010; NEGRÓN JUÁREZ et al., 2007), suggest that the deep soil water storage in the previous wet season can usually provide enough water to maintain the forest evapotranspiration in the subsequent dry period, reducing the impact of the rainfall deficit during dry periods.

Atlantic Forests can also regulate water consumption under drought conditions, since a marked water deficit was not found in the AFR throughout the study period. However, the presence of droughts has considerably affected the AFR hydrological processes, decreasing canopy interception, soil moisture and percolation. On the other hand, the evapotranspiration variability did not follow the growth pattern of secondary tropical forests, which has been documented in other studies (e.g., KUME et al., 2011; VON RANDOW et al., 2020). This fact may be due to (i) the edge effect, preventing its growth and diversification; (ii) the climatic variability; and (iii) the trees' physiological strategies to control water deficit.

In this study, we have analyzed the water balance in the critical zone, considering that the root system up to 1.0 m depth supplies water consumption for this forest ecosystem. However, it is known that some species seek water at deeper layers than 1.0 m. Markewitz et al. (2010) observed that the Amazon forest withdraws water up to 11.5 m depth in dry conditions. This highlight the importance of deep roots in tropical ecosystems to maintain water

use in dry periods (e.g., DA ROCHA et al., 2004; KUME et al., 2011). In this way, further studies should make progress in the hydrological field of Atlantic forests by analyzing the water balance, considering deeper layers and investigating especially deep water percolation. Mello et al. (2019) emphasizes the importance of Atlantic forests for groundwater recharge and soil water storage, showing the resilience of this environment in terms of water yield and maintenance of streamflow during dry periods.

This study presents some limitations and uncertainties that need to be highlighted: (i)  $\Delta S$  was obtained in a monthly step, which precludes the analysis of the temporal variability in shorter scales (e.g., daily), in which water breakthrough is present; (ii) the water balance was carried out solely in the dry periods; (iii) DP was not measured and its calculation was not detailed in daily intervals either; (iv) the critical zone was considered up to 1.0 m depth, which is another source of uncertainty, especially for DP. Many trees species have roots reaching deeper layers in tropical forests (BROEDEL et al., 2017). Regardless of the shortcomings, the analysis highlights the importance of evapotranspiration in the AFR, which was for the first time conducted in forest sites in Brazil throughout seven consecutive hydrological years. These results can potentially improve the understanding of tropical forests under drought conditions and can support decision-makers on better management practices when dealing with Atlantic forest.

## 5 CONCLUSIONS

The results presented in this study show that evapotranspiration is one of the main elements of water balance in forests of Atlantic Forest biome. It presents spatial variability and is an important relationship with soil moisture and weather elements, such as vapor pressure deficit, air temperature and atmospheric pressure. Evapotranspiration is a key element for controlling the hydrological processes, mainly for soil water storage in water constrain periods. The main findings can be summarized as follows:

- a) Net Precipitation accounted for 81% of gross precipitation (P), split into 99.9% throughfall (TF) and 0.1% streamflow. In turn, the canopy rainfall interception was significant in the forest and corresponded to 19% over the period; in the driest hydrological years (from 2014 to 2017), evapotranspiration (E) corresponded to more than 90% of P.

- b) Majority, the hydrological years ended up with a negative soil water storage at 1.0 m in depth in the Atlantic Forest site in the studied period, which was one of the driest ever observed in the region, except in the hydrological years from 2018 to 2020.
- c) The results suggested few spatial variations interannual of evapotranspiration at AFR ( $CV=4.72\%$ ). The evapotranspiration model was able to estimate evapotranspiration on different scales and contribute to the study of the water balance in this forest ecosystem.
- d) In terms of energy balance, evapotranspiration encompassed 60% of net radiation ( $R_n$ ). In the dry seasons, the evapotranspiration was controlled by soil water availability and stomatal controlling regarding the wet seasons, where it was partially controlled by the available energy and atmospheric demand.
- e) Water percolation beneath the root zone (DP) in the studied period did not show capillary rise mainly because of the depth of the Oxisols, being predominantly accounted for percolation. It varied from 3% to 49% of P, showing an expressive reduction in the driest years.

## REFERENCES

- ABDOLGHAFORIAN, A. et al. Characterizing the effect of vegetation dynamics on the bulk heat transfer coefficient to improve variational estimation of surface turbulent fluxes. **Journal of Hydrometeorology**, v. 18, n. 2, p. 321–333, 2017.
- ABDOLLAHI, K.; BAZARGAN, A.; MCKAY, G. **Water Balance Models in Environmental Modeling**. Germany: Springer: Berlin, 2019.
- AGUILOS, M. et al. Interannual and seasonal variations in ecosystem transpiration and water use efficiency in a tropical rainforest. **Forests**, v. 10, n. 1, 2019.
- ALLEN, R. G. et al. **Crop evapotranspiration guidelines for computing crop water requirements**. Rome: FAO, 1998.
- ALVARES, C. A. et al. Köppen's climate classification map for Brazil. **Meteorologische Zeitschrift**, v. 22, n. 6, p. 711–728, 2014.
- BORGES, C. K. et al. Seasonal variation of surface radiation and energy balances over two contrasting areas of the seasonally dry tropical forest (Caatinga) in the Brazilian semi-arid. **Environmental Monitoring and Assessment**, v. 192, n. 8, 2020.
- BROEDEL, E. et al. Deep soil water dynamics in an undisturbed primary forest in central Amazonia: Differences between normal years and the 2005 drought. **Hydrological Processes**, v. 31, n. 9, p. 1749–1759, 2017.
- CABRAL, O. M. R. et al. Water and energy fluxes from a woodland savanna (cerrado) in southeast Brazil. **Journal of Hydrology: Regional Studies**, v. 4, n. PB, p. 22–40, 2015.
- CAMBARDELLA, C. et al. Field-scale variability of soil properties in central Iowa soils. **Soil science society of America journal**, v. 58, n. 5, p. 1501-1511, 1994.
- CHOUDHURY, B. J.; IDSO, S. B.; REGINATO, R. J. Analysis of an empirical model for soil heat flux under a growing wheat crop for estimating evaporation by an infrared-temperature based energy balance equation. **Agricultural and Forest Meteorology**, v. 39, n. 4, p. 283–297, 1987.
- COELHO, C. A. S.; CARDOSO, D. H. F.; FIRPO, M. A. F. Precipitation diagnostics of an exceptionally dry event in São Paulo, Brazil. **Theoretical and Applied Climatology**, v. 125, n. 3–4, p. 769–784, 2016.
- COSTA, M. H. et al. Atmospheric versus vegetation controls of Amazonian tropical rain forest evapotranspiration: Are the wet and seasonally dry rain forests any different? **Journal of Geophysical Research: Biogeosciences**, v. 115, n. 4, p. 1–9, 2010.
- DA ROCHA, H. R. et al. Seasonality of water and heat fluxes over a tropical forest in eastern Amazonia. **Ecological Applications**, v. 14, n. 4 SUPPL., p. 22–32, 2004.
- DA SILVA, D. A. et al. Drivers of leaf area index variation in Brazilian Subtropical Atlantic Forests. **Forest Ecology and Management**, v. 476, p. 118477, 15 nov. 2020.

- ELLISON, D. et al. Trees, forests and water: Cool insights for a hot world. **Global Environmental Change**, v. 43, p. 51–61, 1 mar. 2017.
- ERSHADI, A. et al. Impact of model structure and parameterization on Penman-Monteith type evaporation models. **Journal of Hydrology**, v. 525, p. 521–535, 1 jun. 2015.
- FELTRIN, R. M. et al. Lysimeter soil water balance evaluation for an experiment developed in the Southern Brazilian Atlantic Forest region. **Hydrological Processes**, v. 25, n. 15, p. 2321–2328, 2011.
- FISCHER, M. et al. Evapotranspiration of a high-density poplar stand in comparison with a reference grass cover in the Czech-Moravian Highlands. **Agricultural and Forest Meteorology**, v. 181, p. 43–60, 2013.
- FORD, C. R.; HUBBARD, R. M.; VOSE, J. M. Quantifying structural and physiological controls on variation in canopy transpiration among planted pine and hardwood species in the southern Appalachians. **Ecohydrology**, v. 130, n. February, p. 126–130, 2010.
- FRAGA, C. I. DE M. et al. Condutância do dossel, condutância aerodinâmica e fator de desacoplamento em floresta de Vochysia divergens Pohl (Vochysiaceae) no Pantanal Brasileiro. **Revista Brasileira de Meteorologia**, v. 30, n. 3, p. 275–284, 2015.
- FREITAS, W. K. DE et al. Tree composition of urban public squares located in the Atlantic Forest of Brazil: A systematic review. **Urban Forestry and Urban Greening**, v. 48, n. September 2019, 2020.
- FRIESEN, J.; LUNDQUIST, J.; VAN STAN, J. T. Evolution of forest precipitation water storage measurement methods. **Hydrological Processes**, v. 29, n. 11, p. 2504–2520, 2015.
- G. PYPKER, T.; S. TARASOFF, C.; KOH, H.-S. Assessing the Efficacy of Two Indirect Methods for Quantifying Canopy Variables Associated with the Interception Loss of Rainfall in Temperate Hardwood Forests. **Open Journal of Modern Hydrology**, v. 02, n. 02, p. 29–40, 2012.
- GARRATT, J.; HICKS, B. Momentum, heat and water vapour transfer to and from natural and artificial surfaces. **Quarterly Journal of the Royal Meteorological Society**, v. 99, n. 422, p. 680–687, 1973.
- GENG, J. et al. Dynamics and environmental controls of energy exchange and evapotranspiration in a hilly tea plantation, China. **Agricultural Water Management**, v. 241, n. March, p. 106364, 2020.
- GHIMIRE, C. P. et al. Transpiration and canopy conductance of two contrasting forest types in the Lesser Himalaya of Central Nepal. **Agricultural and Forest Meteorology**, v. 197, p. 76–90, 2014.
- GONG, X. et al. Evapotranspiration partitioning of greenhouse grown tomato using a modified Priestley–Taylor model. **Agricultural Water Management**, v. 247, p. 106709, 31 mar. 2021.
- HAO, Y.; BAIK, J.; CHOI, M. Developing a soil water index-based Priestley–Taylor algorithm for estimating evapotranspiration over East Asia and Australia. **Agricultural and Forest Meteorology**, v. 279, p. 107760, 15 dez. 2019.

- IGARASHI, Y. et al. Environmental control of canopy stomatal conductance in a tropical deciduous forest in northern Thailand. **Agricultural and Forest Meteorology**, v. 202, p. 1–10, 2015.
- IIDA, S. et al. Evapotranspiration from the understory of a tropical dry deciduous forest in Cambodia. **Agricultural and Forest Meteorology**, v. 295, n. September, p. 108170, 2020.
- JARVIS, P. G. The interpretation of the variations in leaf water potential and stomatal conductance found in canopies in the field. **Philosophical Transactions of the Royal Society of London. B, Biological Sciences**, v. 273, n. 927, p. 593–610, 1976.
- JASECHKO, S. et al. Terrestrial water fluxes dominated by transpiration. **Nature**, v. 496, n. 7445, p. 347–350, 2013.
- JASSAL, R. S. et al. Carbon sequestration and water use of a young hybrid poplar plantation in north-central Alberta. **Biomass and Bioenergy**, v. 56, p. 323–333, 1 set. 2013.
- JIAO, L. et al. Determining the independent impact of soil water on forest transpiration: A case study of a black locust plantation in the Loess Plateau, China. **Journal of Hydrology**, v. 572, n. March, p. 671–681, 2019.
- JONES, H. et al. Water balance, surface conductance and water use efficiency of two young hybrid-poplar plantations in Canada's aspen parkland. **Agricultural and Forest Meteorology**, v. 246, n. August 2016, p. 256–271, 2017.
- JUNQUEIRA, J. A. et al. Time-stability of soil water content (SWC) in an Atlantic Forest - Latosol site. **Geoderma**, v. 288, p. 64–78, 2017.
- JUNQUEIRA, J. A. et al. Rainfall partitioning measurement and rainfall interception modelling in a tropical semi-deciduous Atlantic forest remnant. **Agricultural and Forest Meteorology**, v. 275, n. October 2018, p. 170–183, 2019.
- KALMA, J. D.; MCVICAR, T. R.; MCCABE, M. F. Estimating land surface evaporation: A review of methods using remotely sensed surface temperature data. **Surveys in Geophysics**, v. 29, n. 4–5, p. 421–469, 2008.
- KAMALI, M. I. et al. The Determination of Reference Evapotranspiration for Spatial Distribution Mapping Using Geostatistics. **Water Resources Management**, v. 29, n. 11, p. 3929–3940, 2015.
- KANG, M. et al. Energy partitioning and surface resistance of a poplar plantation in northern China. **Biogeosciences**, v. 12, n. 14, p. 4245–4259, 2015.
- KELLIHER, F. M. et al. Maximum conductances for evaporation from global vegetation types. **Agricultural and Forest Meteorology**, v. 73, n. 1–2, p. 1–16, 1995.
- KOOL, D. et al. **A review of approaches for evapotranspiration partitioning** Agricultural and Forest Meteorology Elsevier B.V., , 15 jan. 2014.
- KUME, T. et al. Ten-year evapotranspiration estimates in a Bornean tropical rainforest. **Agricultural and Forest Meteorology**, v. 151, n. 9, p. 1183–1192, 2011.

- LAUNIAINEN, S. et al. Modeling boreal forest evapotranspiration and water balance at stand and catchment scales: a spatial approach. **Hydrology and Earth System Sciences**, v. 23, n. 8, p. 3457–3480, 2019.
- LI, X. et al. A simple and objective method to partition evapotranspiration into transpiration and evaporation at eddy-covariance sites. **Agricultural and Forest Meteorology**, v. 265, n. May 2018, p. 171–182, 2019.
- LI, Z. et al. Evapotranspiration of a tropical rain forest in Xishuangbanna, southwest China. **Hydrological Processes**, v. 24, n. 17, p. 2405–2416, 2010.
- LIU, S. M. et al. Measurements of evapotranspiration from eddy-covariance systems and large aperture scintillometers in the Hai River Basin, China. **Journal of Hydrology**, v. 487, p. 24–38, 22 abr. 2013.
- LOESCHER, H. W. et al. Energy dynamics and modeled evapotranspiration from a wet tropical forest in Costa Rica. **Journal of Hydrology**, v. 315, n. 1–4, p. 274–294, 2005.
- LU, X. et al. Potential of solar-induced chlorophyll fluorescence to estimate transpiration in a temperate forest. **Agricultural and Forest Meteorology**, v. 252, p. 75–87, 15 abr. 2018.
- MA, N. et al. Environmental and biophysical controls on the evapotranspiration over the highest alpine steppe. **Journal of Hydrology**, v. 529, p. 980–992, 2015.
- MACEDO, T. M. et al. Diversity of growth responses to recent droughts reveals the capacity of Atlantic Forest trees to cope well with current climatic variability. **Forest Ecology and Management**, v. 480, p. 118656, 15 jan. 2021.
- MARKEWITZ, D. et al. Soil moisture depletion under simulated drought in the Amazon: Impacts on deep root uptake. **New Phytologist**, v. 187, n. 3, p. 592–607, 2010.
- MARQUES, T. V. et al. Environmental and biophysical controls of evapotranspiration from Seasonally Dry Tropical Forests (Caatinga) in the Brazilian Semiarid. **Agricultural and Forest Meteorology**, v. 287, n. March, 2020.
- MASEYK, K. et al. Physiology – phenology interactions in a productive semi-arid pine forest. n. C, p. 603–616, 2008.
- MCNAUGHTON, K.; JARVIS, P. Predicting effects of vegetation changes on transpiration and evaporation. **Water deficits and plant growth**, v. 7, p. 1-47, 1983.
- MELLO, C. R. et al. Water balance in a neotropical forest catchment of southeastern Brazil. **Catena**, v. 173, n. November 2017, p. 9–21, 2019.
- MELLO, C. R. DE; LIMA, J. M.; SILVA, A. Evapotranspiração em microbacia hidrográfica de fluxo efêmero associada à umidade do solo 1 Evapotranspiration in small ephemeral-watershed associated with soil moisture θ. **Revista Brasileira de Agrometeorologia**, v. 12, n. 1, p. 95–102, 2004.
- MO, X. et al. Simulating temporal and spatial variation of evapotranspiration over the Lushi basin. **Journal of Hydrology**, v. 285, n. 1–4, p. 125–142, 2004.

- MONTEITH, J. L. Evaporation and environment. **Symposia of the Society for Experimental Biology**, n. 19, p. 205–234, 1965.
- MU, Q.; ZHAO, M.; RUNNING, S. W. Improvements to a MODIS global terrestrial evapotranspiration algorithm. **Remote Sensing of Environment**, v. 115, n. 8, p. 1781–1800, 2011.
- MUÑOZ-VILLERS, L. E. et al. Water balances of old-growth and regenerating montane cloud forests in central Veracruz, Mexico. **Journal of Hydrology**, v. 462–463, p. 53–66, 2012.
- MYERS, M. et al. Biodiversity hotspots for conservation priorities. **Nature**, v. 403, n. 2, p. 853–858, 2000.
- NEGRÓN JUÁREZ, R. I. et al. Control of dry season evapotranspiration over the Amazonian forest as inferred from observation at a Southern Amazon forest site. **Journal of Climate**, v. 20, n. 12, p. 2827–2839, 2007.
- NORMAN, J. M.; KUSTAS, W. P.; HUMES, K. S. Source approach for estimating soil and vegetation energy fluxes in observations of directional radiometric surface temperature. **Agricultural and Forest Meteorology**, v. 77, n. 3–4, p. 263–293, 1995.
- OLIVEIRA-FILHO, A. T. et al. **Comparison of the woody flora and soils of six areas of montane semideciduous forest in southern minas gerais, Brazil**. [s.l: s.n.]. v. 51
- OLIVEIRA, P. T. et al. Trends in water balance components across the Brazilian Cerrado. **Water Resources Research**, v. 50, n. 9, p. 7100–7114, 2014.
- PAKPARVAR, M. et al. Artificial recharge efficiency assessment by soil water balance and modelling approaches in a multi-layered vadose zone in a dry region. **Hydrological Sciences Journal**, v. 63, n. 8, p. 1183–1202, 2018.
- PEREIRA, D. et al. Evapotranspiration and estimation of aerodynamic and stomatal conductance in a fragment of Atlantic Forest in Mantiqueira Range Region, MG. **Cerne**, v. 16, p. 32–40, 2010.
- POORTER, L. et al. Biomass resilience of Neotropical secondary forests. **Nature**, v. 530, n. 7589, p. 211–214, 2016.
- PRIESTLEY, C. H. B.; TAYLOR, R. J. On the Assessment of Surface Heat Flux and Evaporation Using Large-Scale Parameters. **Monthly Weather Review**, v. 100, n. 2, p. 81–92, 1972.
- QIU, R. et al. Evapotranspiration estimation using a modified Priestley-Taylor model in a rice-wheat rotation system. **Agricultural Water Management**, v. 224, p. 105755, 1 set. 2019.
- REZENDE, C. L. et al. From hotspot to hopespot: An opportunity for the Brazilian Atlantic Forest. **Perspectives in Ecology and Conservation**, v. 16, n. 4, p. 208–214, 1 out. 2018.
- RODRIGUES, A. **Soil moisture and groundwater recharge prediction in an Atlantic Forest-Oxisol site**. 2019. 67 p. Thesis (Water Resources) - Universidade Federal de Lavras, Lavras, 2019.

- RODRIGUES, A. F. et al. Soil water content and net precipitation spatial variability in an Atlantic forest remnant. **Acta Scientiarum - Agronomy**, v. 42, p. 1–13, 2020.
- SALEMI, L. F. et al. Land-use change in the Atlantic rainforest region: Consequences for the hydrology of small catchments. **Journal of Hydrology**, v. 499, p. 100–109, 2013.
- SANTOS TERRA, M. DE C. N. et al. Stemflow in a neotropical forest remnant: vegetative determinants, spatial distribution and correlation with soil moisture. **Trees - Structure and Function**, v. 32, n. 1, p. 323–335, 2018.
- SCARANO, F. R.; CEOTTO, P. Brazilian Atlantic forest: impact, vulnerability, and adaptation to climate change. **Biodiversity and Conservation**, v. 24, n. 9, p. 2319–2331, 2015.
- SHEIL, D. Forests, atmospheric water and an uncertain future: the new biology of the global water cycle. **Forest Ecosystems**, v. 5, n. 1, 2018.
- SHUTTLEWORTH, W. Observations of radiation exchange above and below Amazonian forest. **Quarterly Journal of the Royal Meteorological Society**, v. 110, n. 466, p. 1163–1169, 1984.
- SHUTTLEWORTH, W. Evaporation from Amazonian rainforest. Proceedings of the Royal society of London. Series B. **Biological sciences**, v. 233, n. 1272, p. 321–346, 1988.
- SILBERSTEIN, R. P. et al. Modelling the energy balance of a natural jarrah (*Eucalyptus marginata*) forest. **Agricultural and Forest Meteorology**, v. 115, n. 3–4, p. 201–230, 2003.
- SU, Z. The Surface Energy Balance System (SEBS) for estimation of turbulent heat fluxes. **Hydrology and Earth System Sciences**, v. 6, n. 1, p. 85–99, 2002.
- TABARI, H.; HOSSEINZADEH TALAEY, P. Sensitivity of evapotranspiration to climatic change in different climates. **Global and Planetary Change**, v. 115, p. 16–23, 1 abr. 2014.
- TAFFARELLO, D. et al. **Hydrological services in the Atlantic Forest, Brazil: An ecosystem-based adaptation using ecohydrological monitoringClimate Services**. Elsevier B.V., , 1 dez. 2017.
- TAMBOSI, L. R. et al. A framework to optimize biodiversity restoration efforts based on habitat amount and landscape connectivity. **Restoration Ecology**, v. 22, n. 2, p. 169–177, 2014.
- TAN, Z. H. et al. Surface conductance for evapotranspiration of tropical forests: Calculations, variations, and controls. **Agricultural and Forest Meteorology**, v. 275, n. June, p. 317–328, 2019.
- TOMASELLA, J. et al. The water balance of an Amazonian micro-catchment: the effect of interannual variability of rainfall on hydrological behaviour. **Hydrological Processes**, v. 2274, n. November 2008, p. 2267–2274, 2008.
- TOR-NGERN, P. et al. Water balance of pine forests: Synthesis of new and published results. **Agricultural and Forest Meteorology**, v. 259, n. April, p. 107–117, 2018.
- USDA. **Soil taxonomy: a basic system of soil classification for making and interpreting soil surveys**. Washington, DC., 1975.

VON RANDOW, R. DE C. S. et al. Evapotranspiration and gross primary productivity of secondary vegetation in Amazonia inferred by eddy covariance. **Agricultural and Forest Meteorology**, v. 294, p. 108141, 15 nov. 2020.

YAN, C. et al. Effects of forest evapotranspiration on soil water budget and energy flux partitioning in a subalpine valley of China. **Agricultural and Forest Meteorology**, v. 246, n. June, p. 207–217, 2017.

ZANINI, A. M. et al. The effect of ecological restoration methods on carbon stocks in the Brazilian Atlantic Forest. **Forest Ecology and Management**, v. 481, n. November 2020, p. 118734, 2021.

ZHAO, L. et al. Evapotranspiration estimation methods in hydrological models. **Journal of Geographical Sciences**, v. 23, n. 2, p. 359–369, 2013.

ZHAO, W. et al. Evapotranspiration partitioning, stomatal conductance, and components of the water balance: A special case of a desert ecosystem in China. **Journal of Hydrology**, v. 538, p. 374–386, 2016.

ZHENG, H. et al. Spatial variation in annual actual evapotranspiration of terrestrial ecosystems in China: Results from eddy covariance measurements. **Journal of Geographical Sciences**, v. 26, n. 10, p. 1391–1411, 2016.

## APÊNDICES

### APÊNDICE A – Variáveis complementares do modelo PM

A parametrização das variáveis complementares do modelo Penman-Monteith (PM) foram calculadas com base em ALLEN et al. (1998):

O déficit de pressão de vapor d' água (VPD, em kPa) foi calculado como:

$$\text{VPD} = e_s - e_a \quad (1)$$

A pressão de saturação de vapor d' água ( $e_s$ , em kPa), foi estimada com a  $T_a$  ( $^{\circ}\text{C}$ ), assim:

$$e_s = 0.6108 \cdot \exp\left(\frac{17.27 \cdot T_a}{T_a + 237.3}\right) \quad (2)$$

A pressão atual de vapor d' água ( $e_a$ , em kPa), foi dada por:

$$e_a \text{ (kPa)} = \frac{\text{RH} \cdot e_s}{100} \quad (3)$$

A declividade da curva de pressão de saturação de vapor ( $\Delta$ , em  $\text{kPa } ^{\circ}\text{C}^{-1}$ ) foi estimada assim:

$$\Delta = \frac{4098 \cdot e_s}{(237.3 + T_a)^2} \quad (4)$$

O coeficiente psicrométrico ( $\gamma$ , em  $\text{kPa } ^{\circ}\text{C}^{-1}$ ) pode ser obtido pela seguinte equação:

$$\gamma = 0.0016286 \cdot \frac{P_a}{\lambda} \quad (5)$$

em que  $P_a$  é a pressão atmosférica (kPa) e  $\lambda$  é o calor latente de vaporização da água ( $\text{MJ Kg}^{-1} ^{\circ}\text{C}^{-1}$ ).

## REFERÊNCIAS

ALLEN, R. G. et al. **Crop evapotranspiration guidelines for computing crop water requirements.** Rome: FAO, 1998.